Paulo Roberto de Jesus Dantas

Mathematical Modeling of Curved Rectangular Waveguides using the Variational Rayleigh-Ritz Method

Dissertação de Mestrado

Rio de Janeiro
April 2023

Paulo Roberto de Jesus Dantas

Mathematical Modeling of Curved Rectangular Waveguides using the Variational Rayleigh-Ritz Method

Thesis presented to the Programa de Pós–graduação em Engenharia de Elétrica da PUC-Rio in partial fulfillment of the requirements for the degree of Mestre em Engenharia de Elétrica. Approved by the Examination Committee:

Prof. Guilherme Simon da Rosa
Advisor
Departamento de Engenharia Elétrica – PUC-Rio

Prof. Rafael Abrantes Penchel
Universidade Estadual Paulista – UNESP

Prof. José Ricardo Begmann
Departamento de Engenharia Elétrica – PUC-Rio

Rio de Janeiro, April the 27th, 2023

Paulo Roberto de Jesus Dantas

Majored in Curso Superior de Tecnologia em Sistemas de Telecomunicações no Instituto Federal de Educação, Ciência e Tecnologia Sul-rio-grandense

To my parents
and my son.

Acknowledgments

I would like firstly thank PUC-Rio and all professors of the Programa de Pós-Graduação em Engenharia Elétrica that taught me specially my advisor, Guilherme Simon da Rosa, for the support, guidance and suggestions and also for his personal generosity that helped me and encouraged me in the bad moments.

My deep gratitude to my family and friends that also supported me in this journey. I am especially grateful to my friends Ricardo that introduced me to the PUC's postgraduate program and Marcello for the support, encouragement and valuable discussions.

Abstract

de Jesus Dantas, Paulo Roberto; Simon da Rosa, Guilheme (Advisor). **Mathematical Modeling of Curved Rectangular Waveguides using the Variational Rayleigh-Ritz Method**. Rio de Janeiro, 2023. 50p. Dissertação de Mestrado – Departamento de Engenharia Elétrica, Pontifícia Universidade Católica do Rio de Janeiro.

This study presents a computational method for modeling electromagnetic fields in curved rectangular waveguides with uniform cross-section, using the variational Rayleigh-Ritz method. The potential applications of this research in engineering include the design of feeders for antennas, microwave mode converter devices, filters, among others. While various models have been proposed to solve this problem, conventional numerical techniques based on finite elements, finite differences, and finite volumes require high computational costs. To overcome these issues, a variational formulation for solving Maxwell's equations in a local toroidal coordinate system was developed via a novel functional introduced in this work. The functional was adapted to handle uniformly bend domains with arbitrary cross-section, and analytical investigations were conducted to confirm its stationary characteristics. The Rayleigh-Ritz formalism was employed to convert the functional into an equivalent problem of eigenvalues and eigenvectors using an expansion in terms of rectangular harmonics of a straight waveguide as basis functions for modeling a bend rectangular waveguide. A numerical algorithm was developed in Matlab to validate our model, and the results were compared against reference perturbational and numerical solutions, demonstrating high accuracy and lower computational costs.

Keywords

Curved Rectangular Waveguides; Rayleigh-Ritz Method; Variational; Mathematical Modeling; Toroidal Coordinate.

Resumo

de Jesus Dantas, Paulo Roberto; Simon da Rosa, Guilheme. **Modelagem Matemática de Guias de Onda Retangulares Curvados usando o Método Variacional de Rayleigh-Ritz**. Rio de Janeiro, 2023. 50p. Dissertação de Mestrado – Departamento de Engenharia Elétrica, Pontifícia Universidade Católica do Rio de Janeiro.

Este estudo apresenta um método computacional para modelar campos eletromagnéticos em guias de onda retangulares curvados com seção transversal uniforme, usando o método variacional de Rayleigh-Ritz. Potenciais aplicações desta pesquisa em engenharia incluem o projeto de alimentadores para antenas, conversores de modais na faixa de micro-ondas, filtros, entre outros. Embora vários modelos tenham sido propostos para resolver este problema, as técnicas numéricas convencionais baseadas em elementos finitos, diferenças finitas e volumes finitos requerem altos custos computacionais. Para superar esses problemas, foi desenvolvida uma formulação variacional para resolver as equações de Maxwell em um sistema de coordenadas toroidal local, por meio de um novo funcional introduzido neste trabalho. O funcional foi adaptado para domínios uniformemente curvados com seção transversal arbitrária, e investigações analíticas foram conduzidas para confirmar suas características estacionárias. O formalismo Rayleigh-Ritz foi utilizado para converter o funcional em um problema equivalente de autovalores e autovetores, usando uma expansão em harmônicas retangulares de um guia de onda reto como funções de base para modelar um guia de onda retangular curvo. Um algoritmo numérico foi desenvolvido em Matlab para validar nosso modelo, e os resultados foram comparados com soluções perturbacionais e numéricas de referência, demonstrando alta precisão e menor custo computacional.

Palavras-chave

Guias de onda retangulares curvados; Método de Rayleigh-Ritz; Formulação variacional; Modelagem matemática; Coordenadas Toroidal.

Table of contents

List of figures

List of tables

1
Introduction

1.1
General Introduction

The advancement of technology in electrical engineering, coupled with the use of high-frequency systems, has resulted in an increasing demand for compact devices that can propagate guided waves in curved structures as depicted in Fig. 1.1. In this case, curved rectangular waveguides where used to make connections in a complex microwave device.

Uniform bend rectangular waveguides are commonly used in microwave device applications. To analyze the boundary-value problem associated with these waveguides, cylindrical harmonics can be used to derive characteristic equations for transverse electric (TE) and magnetic (TM) modes [1]. The problem is typically formulated for E- and H-plane bend waveguide configurations, and determining the modal fields requires solving non-linear eigenvalue problems that involve finding the zeros of transcendental equations with cross-product combinations of Bessel functions. Zero-finding algorithms are typically used to solve these equations [2, Sec. 8.1]. The eigenvalues that must be found correspond to the orders of Bessel and Neumann functions.
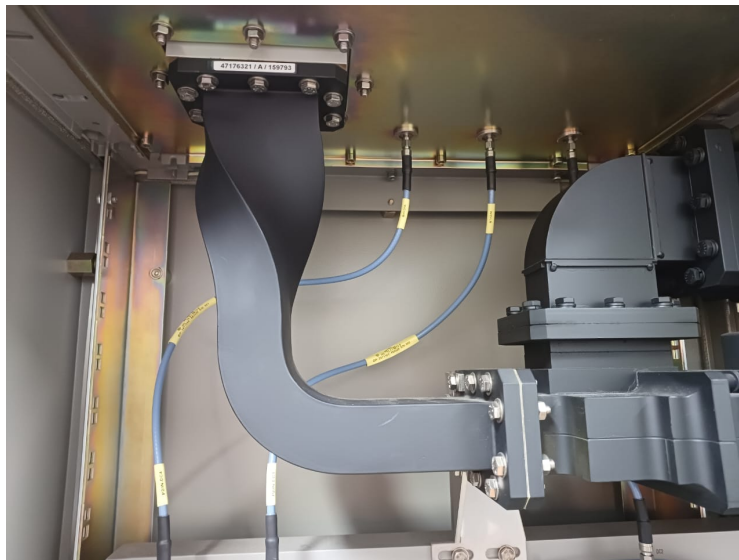
Figure 1.1: Curved rectangular waveguides of Radar TA10.

However, as the radius of curvature R of the waveguide (refer to Fig. 2.1) increases, the absolute values of the proper eigenvalues also increase, which poses a significant challenge for conventional numerical libraries that compute cylindrical functions.

The study in [3] provides approximate formulas for the fundamental propagating modes (which correspond to large real orders of cylindrical functions) for large values of R. However, numerical problems such as underflow and overflow can arise when solving for imaginary eigenvalues. This issue led to the investigation of asymptotic approximations for Bessel functions of imaginary orders in [4].

While the techniques outlined in [3, 4] can help to avoid ill-conditioned equations, it is important to carefully consider the trade-off between accuracy and computational efficiency, especially in scenarios where R is not sufficiently large.

In [2, Ch.4], a local coordinate system was used to express Maxwell's equations, which includes a 2D Cartesian coordinate system and an orthogonal curved longitudinal axis. The corresponding Helmholtz wave equations were then solved by expanding the field solutions in a series of inverse powers of the radius of curvature (R^{-1}). This perturbation solution method produced zeroth-order fields and propagating constants that resemble those of a straight rectangular waveguide. First- and second-order corrections were obtained in [2] by solving differential equations associated with the coefficients R^{-1} and R^{-2}, respectively.

In a similar fashion, a perturbation approach was used in [5] to model curved microstrip bend transmission lines.

Furthermore, the mode-coupling theory can be employed to take into account the effects of bends in rectangular waveguides. For instance, in [6], the coupled-mode approach was used to analyze the fields in curved and twisted waveguides.

The method of local modes was used to analyze E-plane and H-plane bend waveguides in [7]. In this method, the field in a curved waveguide section is expressed as a superposition of modes of the locally straight waveguide. The modal coupling is then described by a system of generalized telegrapher's equations.

The authors of [8] introduced a multimode equivalent network model for the analysis of uniform E-plane and H-plane bends in rectangular waveguides.

The method of moments (MoM) has been employed in several works for rigorously describing the propagation in bent waveguides. For instance, in [9], a combined MoM and mode-matching technique was used for the analysis of

curved parallel-plate waveguides.

In [10], a method was proposed for modeling waveguide bends by cascading sections of straight rectangular waveguides. The resulting system of coupled ordinary differential equations for the field components was then solved using the MoM. The accuracy of the method was validated by comparing the computed electromagnetic propagation in bent waveguides with experimental results.

The work in [11] presents a finite-difference-based approach for modeling curved waveguides by discretizing Maxwell's equations in orthogonal curvilinear coordinates. This approach, which is free of staircase effects, was used for the eigenvalue analysis of curved waveguides in the frequency domain. The method is capable of avoiding the need for a fine mesh, which is advantageous for modeling highly curved structures.

Recently, in [12], a novel scaling procedure that stabilizes Bessel functions of the exact boundary-value problem of a bent rectangular waveguide. This work presents new scaled representations for Hankel functions of first and second kinds into a numerically stable representation that accurately describe the behavior of electromagnetic fields in curved rectangular waveguides using double-precision floating-point arithmetic. Besides that, the solution is limited to lossless waveguides.

At higher frequencies, curved dielectric waveguides are fundamental building blocks in many optical devices [13]. The analysis of optical waveguide bends can be accomplished using modified versions of the methods described above. In particular, reliable solutions can be achieved when the curved waveguide is treated as an equivalent straight waveguide approximation [14]. More accuracy can be provided by vectorial meshless-based methods [15] or via transformation optics principles assisted by the FEM [16].

In [1], a variational method for solving Maxwell's equations in straight waveguides is presented. Improvements of this approach are shown in [17].

To the best of our knowledge, there are no semi-analytic methods to characterize field propagation in rectangular waveguides that are: a) adequate for modeling small curvature scenarios, b) do not require complex-tailored special functions, c) proof against spurious modes, and d) allow the modeling of lossy waveguide scenarios. This led us to develop a variational formulation of Maxwell's equations using the Rayleigh-Ritz method in the toroidal coordinate system, which offers a more efficient solution to this problem than conventional numerical techniques such as finite elements, differences, or finite volumes. This research is significant in the field of engineering because it offers potential applications in the design of feeders for antennas and microwave devices, filters,

and other related devices.

The analytical and computational methodology developed in this study provides a means of modeling electromagnetic fields in toroidal coordinates of curved rectangular waveguides with uniform cross-section, using a variational formula via the Rayleigh-Ritz method. The functional obtained from this methodology was adapted to handle boundary conditions in rectangular cross-sectional waveguides, and analytical investigations were conducted to confirm the stationary characteristics of the functional. An expansion in terms of complete eigenfunctions was used to convert the functional into an equivalent problem of eigenvalues and eigenvectors. A numerical algorithm was developed to validate the technique, and the results were compared to reference solutions in several representative cases. The proposed methodology achieved good accuracy while requiring a lower computational cost, making it an attractive option for researchers and engineers in the field of electrical engineering.

1.2
Scientific Contributions

The scientific contributions of this work are listed bellow:

– Development of a variational formula in toroidal coordinates for modeling curved waveguides with uniform cross-section.

– Development of an analytical and computational methodology for modeling electromagnetic fields in toroidal coordinates of curved rectangular waveguides with uniform cross-section, utilizing the presented variational formula via the Rayleigh-Ritz method.

– Introduction of a variational formulation capable of characterizing waveguides filled with lossy media, which is not possible using the semi-analytic method presented in [12].

1.3
Dissertation Organization

The rest of this dissertation is organized as follows. In Chapter 2, we present the development of a variational formula in toroidal coordinates for modeling curved waveguides with uniform cross-section, and its solution via the Rayleigh-Ritz method.

In Chapter 3, we describe an analytical and computational methodology for modeling electromagnetic fields in waveguides with uniform cross-section in toroidal coordinates, using the Rayleigh-Ritz method to solve for a H-plane bend.

Finally, in Chapter 4, we conclude with a summary of our findings and suggestions for future research directions.

2
Variational Formulation

2.1
Variational Formula for Waveguides with Curved Longitudinal Axis

In what follows, we adopt a notation similar to that in [1], where the time-harmonic dependence in the form $\exp(+j\omega t)$ is assumed and omitted. Maxwell's curls equation in an isotropic media can be written as

$$-\boldsymbol{\nabla} \times \mathbf{E} = j\omega\mu\,\mathbf{H} + \mathbf{M} \tag{2-1}$$

$$\boldsymbol{\nabla} \times \mathbf{H} = j\omega\epsilon\,\mathbf{E} + \mathbf{J}. \tag{2-2}$$

We consider the geometry of a uniform bend waveguide with a constant radius of curvature R depicted in Fig. 2.1, where the longitudinal direction refers to the ζ-axis. The waveguide cross-section can either be described in terms of the 2D Cartesian coordinates (x, y) or its polar correspondent (ρ, ϕ). The forward and backward ζ-traveling waves are associated with the electric and magnetic fields

$$\begin{aligned}\mathbf{E}^{\pm} &= \mathbf{e}^{\pm}(\rho, \phi)\,e^{\mp jk_\zeta\zeta} \\ &= [\mathbf{e}_t(\rho, \phi) \pm \mathbf{u}_\zeta\,e_\zeta(\rho, \phi)]\,e^{\mp jk_\zeta\zeta}, \\ \mathbf{H}^{\pm} &= \mathbf{h}^{\pm}(\rho, \phi)\,e^{\mp jk_\zeta\zeta} \\ &= [\pm\mathbf{h}_t(\rho, \phi) + \mathbf{u}_\zeta\,h_\zeta(\rho, \phi)\,e^{\mp jk_\zeta\zeta}],\end{aligned} \tag{2-3} \tag{2-4}$$

for $\zeta \gtrless 0$. In the above, the subscripts ζ and t are used to describe axial (along ζ) and transversal (to ζ) components, respectively. A unit vector pointing to the α-direction is denoted as $\mathbf{u}_\alpha$, where α can be any direction in a coordinate system.

By substituting (2-3) and (2-4) into (2-1) and (2-2), we obtain for the $+\zeta$ traveling wave

$$-\boldsymbol{\nabla} \times (\mathbf{e}^{+}\,e^{-jk_\zeta\zeta}) = j\omega\mu\,\mathbf{h}^{+}\,e^{-jk_\zeta\zeta} + \mathbf{M}, \tag{2-5}$$

$$\boldsymbol{\nabla} \times (\mathbf{h}^{+}\,e^{-jk_\zeta\zeta}) = j\omega\epsilon\,\mathbf{e}^{+}\,e^{-jk_\zeta\zeta} + \mathbf{J}. \tag{2-6}$$

Note that the (ρ, ϕ) dependence was omitted in the above expressions for
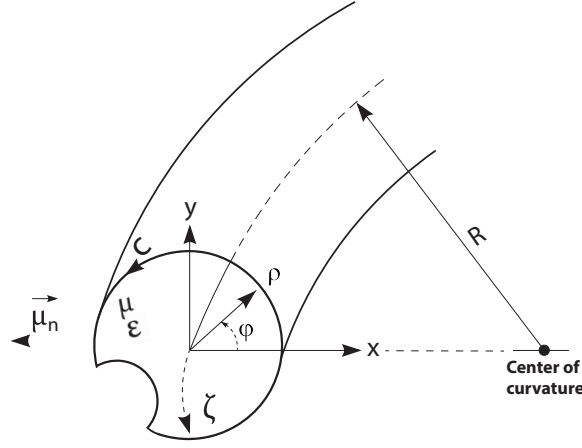
Figure 2.1: Geometry of a curved waveguide with an arbitrary cross section.

simplicity. By writing the nabla operator as $\boldsymbol{\nabla} = \boldsymbol{\nabla}_t + \mathbf{u}_\zeta \, \nabla_\zeta$, where

$$\boldsymbol{\nabla}_t = \mathbf{u}_\rho \, \frac{\partial}{\partial \rho} + \mathbf{u}_\phi \, \frac{1}{\rho} \, \frac{\partial}{\partial \phi}, \tag{2-7}$$

$$\nabla_\zeta = \frac{1}{h} \, \frac{\partial}{\partial \zeta}, \tag{2-8}$$

with the metric coefficient of the ζ-direction is given by $h = 1 - R^{-1} \rho \, \cos(\phi)$ [18, App. C], [19], we obtain

$$-(\boldsymbol{\nabla}_t + \mathbf{u}_\zeta \nabla_\zeta) \times [(\mathbf{e}_t^+ + \mathbf{u}_\zeta \, e_\zeta^+) \, e^{-jk_\zeta \zeta}] = j\omega\mu \, \mathbf{h}^+ \, e^{-jk_\zeta \zeta} + \mathbf{M}, \tag{2-9}$$

$$(\boldsymbol{\nabla}_t + \mathbf{u}_\zeta \nabla_\zeta) \times [(\mathbf{h}_t^+ + \mathbf{u}_\zeta \, h_\zeta^+) \, e^{-jk_\zeta \zeta}] = j\omega\epsilon \, \mathbf{e}^+ \, e^{-jk_\zeta \zeta} + \mathbf{J}. \tag{2-10}$$

The above has the extended forms

$$-\left(\boldsymbol{\nabla}_t \times \mathbf{e}_t^+ + \boldsymbol{\nabla}_t \times \mathbf{u}_\zeta \, e_\zeta^+ + \mathbf{u}_\zeta \nabla_\zeta \times \mathbf{e}_t^+ + \mathbf{u}_\zeta \nabla_\zeta \times \mathbf{u}_\zeta \, e_\zeta^+\right) e^{-jk_\zeta \zeta} =$$
$$+ j\omega\mu \, \mathbf{h}^+ \, e^{-jk_\zeta \zeta} + \mathbf{M}, \quad \text{(2-11)}$$

$$\left(\boldsymbol{\nabla}_t \times \mathbf{h}_t^+ + \boldsymbol{\nabla}_t \times \mathbf{u}_\zeta \, h_\zeta^+ + \mathbf{u}_\zeta \, \nabla_\zeta \times \mathbf{h}_t^+ + \mathbf{u}_\zeta \, \nabla_\zeta \times \mathbf{u}_\zeta \, h_\zeta^+\right) e^{-jk_\zeta \zeta} =$$
$$+ j\omega\epsilon \, \mathbf{e}^+ \, e^{-jk_\zeta \zeta} + \mathbf{J}. \quad \text{(2-12)}$$

Since ∇_ζ is a function of (ρ, ϕ) and $\mathbf{u}_\zeta$ is not a constant vector, the terms $\mathbf{u}_\zeta \, \nabla_\zeta \times \mathbf{e}_t^+ \, e^{-jk_\zeta \zeta}$ and $\mathbf{u}_\zeta \, \nabla_\zeta \times \mathbf{u}_\zeta \, e_\zeta^+ \, e^{-jk_\zeta \zeta}$ need to be further investigated once there are no obvious simplifications as in the curvature-vanishing special scenario in which $R^{-1} \to 0$.

We found:

$$\mathbf{u}_\zeta \, \nabla_\zeta \times \mathbf{e}_t \, e^{-jk_\zeta \zeta} = \mathbf{u}_\zeta \, h^{-1} \frac{\partial}{\partial \zeta} \times \mathbf{e}_t \, e^{-jk_\zeta \zeta} \tag{2-13}$$

$$= \mathbf{u}_\zeta \, h^{-1} \times \frac{\partial}{\partial \zeta} \left(\mathbf{u}_\rho \, e_\rho \, e^{-jk_\zeta \zeta} + \mathbf{u}_\phi \, e_\phi \, e^{-jk_\zeta \zeta} \right) \tag{2-14}$$

$$= \mathbf{u}_\zeta \, h^{-1} \times \left[e_\rho \frac{\partial}{\partial \zeta} \left(\mathbf{u}_\rho \, e^{-jk_\zeta \zeta} \right) + e_\phi \frac{\partial}{\partial \zeta} \left(\mathbf{u}_\phi \, e^{-jk_\zeta \zeta} \right) \right] \tag{2-15}$$

$$= \mathbf{u}_\zeta \, h^{-1} \times \left[e_\rho \left(\mathbf{u}_\rho \frac{\partial}{\partial \zeta} e^{-jk_\zeta \zeta} + e^{-jk_\zeta \zeta} \frac{\partial}{\partial \zeta} \mathbf{u}_\rho \right) \right.$$
$$\left. + e_\phi \left(\mathbf{u}_\phi \frac{\partial}{\partial \zeta} e^{-jk_\zeta \zeta} + e^{-jk_\zeta \zeta} \frac{\partial}{\partial \zeta} \mathbf{u}_\phi \right) \right] \tag{2-16}$$

$$= \mathbf{u}_\zeta \, h^{-1} \times \left[e_\rho \left(\mathbf{u}_\rho \, (-jk_\zeta) \, e^{-jk_\zeta \zeta} + e^{-jk_\zeta \zeta} \, \mathbf{u}_\zeta \frac{\partial h}{\partial \rho} \right) \right.$$
$$\left. + e_\phi \left(\mathbf{u}_\phi \, (-jk_\zeta) \, e^{-jk_\zeta \zeta} + e^{-jk_\zeta \zeta} \, \mathbf{u}_\zeta \, \rho^{-1} \frac{\partial h}{\partial \phi} \right) \right] \tag{2-17}$$

$$= -jk_\zeta \, h^{-1} \, \mathbf{u}_\zeta \times (\mathbf{u}_\rho \, e_\rho + \mathbf{u}_\phi \, e_\phi) \, e^{-jk_\zeta \zeta} \tag{2-18}$$

$$= -jk_\zeta \, h^{-1} \, \mathbf{u}_\zeta \times \mathbf{e}_t \, e^{-jk_\zeta \zeta}. \tag{2-19}$$

Notice in the above we have used that the unit vectors $\mathbf{u}_\rho$ and $\mathbf{u}_\phi$ are independent of ζ, and that $\partial \mathbf{u}_\rho / \partial \zeta = \mathbf{u}_\zeta \, \partial h / \partial \rho$ and $\partial \mathbf{u}_\phi / \partial \zeta = \mathbf{u}_\zeta \, \rho^{-1} \, \partial h / \partial \phi$ [19, App. A].

In addition, we have found:

$$\mathbf{u}_\zeta \, \nabla_\zeta \times \mathbf{u}_\zeta \, e_\zeta \, e^{-jk_\zeta \zeta} = \mathbf{u}_\zeta \, h^{-1} \frac{\partial}{\partial \zeta} \times \mathbf{u}_\zeta \, e_\zeta \, e^{-jk_\zeta \zeta} \tag{2-20}$$

$$= h^{-1} \, e_\zeta \, \mathbf{u}_\zeta \times \left(\mathbf{u}_\zeta \frac{\partial}{\partial \zeta} e^{-jk_\zeta \zeta} + e^{-jk_\zeta \zeta} \frac{\partial}{\partial \zeta} \mathbf{u}_\zeta \right) \tag{2-21}$$

$$= h^{-1} \, e_\zeta \, e^{-jk_\zeta \zeta} \, \mathbf{u}_\zeta \times \frac{\partial}{\partial \zeta} \mathbf{u}_\zeta \tag{2-22}$$

$$= h^{-1} \, e_\zeta \, e^{-jk_\zeta \zeta} \, \mathbf{u}_\zeta \times (R^{-1} \, \mathbf{u}_x) \tag{2-23}$$

$$= \mathbf{u}_y \, R^{-1} \, h^{-1} \, e_\zeta \, e^{-jk_\zeta \zeta} \tag{2-24}$$

$$= [\mathbf{u}_\rho \, \sin(\phi) + \mathbf{u}_\phi \, \cos(\phi)] \, R^{-1} \, h^{-1} \, e_\zeta \, e^{-jk_\zeta \zeta}. \tag{2-25}$$

In the above, we used $\partial \mathbf{u}_\zeta / \partial \zeta = R^{-1} \, \mathbf{u}_x$.

Now, by multiplying (2-11) and (2-12) by $e^{+jk_\zeta \zeta}$, with the help of (2-19) and (2-25), we obtain

$$\boldsymbol{\nabla}_t \times \mathbf{e}_t^+ + \boldsymbol{\nabla}_t \times \mathbf{u}_\zeta \, e_\zeta^+ - jk_\zeta \, h^{-1} \, \mathbf{u}_\zeta \times \mathbf{e}_t^+ + \mathbf{u}_y \, R^{-1} \, h^{-1} \, e_\zeta^+ =$$

$$- j\omega\mu\,\mathbf{h}^+ - \mathbf{M}\,e^{+jk_\zeta\zeta}, \quad (2\text{-}26)$$

$$\boldsymbol{\nabla}_t \times \mathbf{h}_t^+ + \boldsymbol{\nabla}_t \times \mathbf{u}_\zeta\,h_\zeta^+ - jk_\zeta\,h^{-1}\,\mathbf{u}_\zeta \times \mathbf{h}_t^+ + \mathbf{u}_y\,R^{-1}\,h^{-1}\,h_\zeta^+ =$$
$$+ j\omega\epsilon\,\mathbf{e}^+ + \mathbf{J}\,e^{+jk_\zeta\zeta}. \quad (2\text{-}27)$$

Analogously, for $-\zeta$ traveling wave, there exist equations dual to (2-26) and (2-27), i.e.,

$$\boldsymbol{\nabla}_t \times \mathbf{e}_t^- + \boldsymbol{\nabla}_t \times \mathbf{u}_\zeta\,e_\zeta^- + jk_\zeta\,h^{-1}\,\mathbf{u}_\zeta \times \mathbf{e}_t^- + \mathbf{u}_y\,R^{-1}\,h^{-1}\,e_\zeta^- =$$
$$- j\omega\mu\,\mathbf{h}^- - \mathbf{M}\,e^{-jk_\zeta\zeta}, \quad (2\text{-}28)$$

$$\boldsymbol{\nabla}_t \times \mathbf{h}_t^- + \boldsymbol{\nabla}_t \times \mathbf{u}_\zeta\,h_\zeta^- + jk_\zeta\,h^{-1}\,\mathbf{u}_\zeta \times \mathbf{h}_t^- + \mathbf{u}_y\,R^{-1}\,h^{-1}\,h_\zeta^- =$$
$$+ j\omega\epsilon\,\mathbf{e}^- + \mathbf{J}\,e^{-jk_\zeta\zeta}. \quad (2\text{-}29)$$

Now, by dot-multiplying (2-26) with $\mathbf{h}^-$, and (2-29) with $\mathbf{e}^+$, we obtain

$$\mathbf{h}^- \cdot \boldsymbol{\nabla}_t \times \mathbf{e}_t^+ + \mathbf{h}^- \cdot \boldsymbol{\nabla}_t \times \mathbf{u}_\zeta\,e_\zeta^+ - jk_\zeta\,h^{-1}\,\mathbf{h}^- \cdot \mathbf{u}_\zeta \times \mathbf{e}_t^+ + \mathbf{h}^- \cdot \mathbf{u}_y\,R^{-1}\,h^{-1}\,e_\zeta^+ =$$
$$- j\omega\mu\,\mathbf{h}^- \cdot \mathbf{h}^+ - \mathbf{h}^- \cdot \mathbf{M}\,e^{+jk_\zeta\zeta}, \quad (2\text{-}30)$$

$$\mathbf{e}^+ \cdot \boldsymbol{\nabla}_t \times \mathbf{h}_t^- + \mathbf{e}^+ \cdot \boldsymbol{\nabla}_t \times \mathbf{u}_\zeta\,h_\zeta^- + jk_\zeta\,h^{-1}\,\mathbf{e}^+ \cdot \mathbf{u}_\zeta \times \mathbf{h}_t^- + \mathbf{e}^+ \cdot \mathbf{u}_y\,R^{-1}\,h^{-1}\,h_\zeta^- =$$
$$+ j\omega\epsilon\,\mathbf{e}^+ \cdot \mathbf{e}^- + \mathbf{e}^+ \cdot \mathbf{J}\,e^{-jk_\zeta\zeta}. \quad (2\text{-}31)$$

Adding the last two equations yields

$$\mathbf{h}^- \cdot \boldsymbol{\nabla}_t \times \mathbf{e}_t^+ + \mathbf{e}^+ \cdot \boldsymbol{\nabla}_t \times \mathbf{h}_t^- + \mathbf{h}^- \cdot \boldsymbol{\nabla}_t \times \mathbf{u}_\zeta\,e_\zeta^+ + \mathbf{e}^+ \cdot \boldsymbol{\nabla}_t \times \mathbf{u}_\zeta\,h_\zeta^-$$
$$- jk_\zeta\,h^{-1}\,(\mathbf{h}^- \cdot \mathbf{u}_\zeta \times \mathbf{e}_t^+ - \mathbf{e}^+ \cdot \mathbf{u}_\zeta \times \mathbf{h}_t^-) + R^{-1}\,h^{-1}(h_y^-\,e_\zeta^+ + e_y^+\,h_\zeta^-) =$$
$$- j\omega\mu\,\mathbf{h}^- \cdot \mathbf{h}^+ + j\omega\epsilon\,\mathbf{e}^+ \cdot \mathbf{e}^- - \mathbf{h}^- \cdot \mathbf{M}\,e^{+jk_\zeta\zeta} + \mathbf{e}^+ \cdot \mathbf{J}\,e^{-jk_\zeta\zeta}. \quad (2\text{-}32)$$

By using the circular-shift invariance of scalar triple product, we can verify that

$$\mathbf{h}^- \cdot \mathbf{u}_\zeta \times \mathbf{e}_t^+ = -\mathbf{e}_t^+ \cdot \mathbf{u}_\zeta \times \mathbf{h}^-. \quad (2\text{-}33)$$

Also, by noticing that only transverse field components contribute to the above,

we can verify that

$$\mathbf{h}^- \cdot \mathbf{u}_\zeta \times \mathbf{e}_t^+ - \mathbf{e}^+ \cdot \mathbf{u}_\zeta \times \mathbf{h}_t^- = -2\left(\mathbf{e}_t^+ \times \mathbf{h}_t^+\right) \cdot \mathbf{u}_\zeta, \qquad (2\text{-}34)$$

because $\mathbf{h}_t^- = -\mathbf{h}_t^+$. If we now define the source-like terms $\mathbf{M} = \mathbf{m}^+(\rho, \phi)\, e^{-jk_\zeta \zeta}$ and $\mathbf{J} = \mathbf{j}^-(\rho, \phi)\, e^{+jk_\zeta \zeta}$, we can rearrange (2-32) to obtain

$$\mathbf{h}^- \cdot \boldsymbol{\nabla}_t \times \mathbf{e}_t^+ + \mathbf{e}^+ \cdot \boldsymbol{\nabla}_t \times \mathbf{h}_t^- + \mathbf{h}^- \cdot \boldsymbol{\nabla}_t \times \mathbf{u}_\zeta\, e_\zeta^+ + \mathbf{e}^+ \cdot \boldsymbol{\nabla}_t \times \mathbf{u}_\zeta\, h_\zeta^-$$
$$+ R^{-1}\, h^{-1}(h_y^-\, e_\zeta^+ + e_y^+\, h_\zeta^-) + j\omega\mu\, \mathbf{h}^- \cdot \mathbf{h}^+ - j\omega\epsilon\, \mathbf{e}^+ \cdot \mathbf{e}^- + \mathbf{h}^- \cdot \mathbf{m}^+ - \mathbf{e}^+ \cdot \mathbf{j}^-$$
$$= -2jk_\zeta\, h^{-1}\left(\mathbf{e}_t^+ \times \mathbf{h}_t^+\right) \cdot \mathbf{u}_\zeta. \quad (2\text{-}35)$$

Recalling that $\mathbf{e}^+ = \mathbf{e}_t^+ + \mathbf{u}_\zeta\, e_\zeta^+$ and $\mathbf{h}^- = \mathbf{h}_t^- + \mathbf{u}_\zeta\, h_\zeta^-$, we can reduces (2-35) to

$$\mathbf{h}^- \cdot \boldsymbol{\nabla}_t \times \mathbf{e}^+ + \mathbf{e}^+ \cdot \boldsymbol{\nabla}_t \times \mathbf{h}^- + j\omega\mu\, \mathbf{h}^- \cdot \mathbf{h}^+ - j\omega\epsilon\, \mathbf{e}^+ \cdot \mathbf{e}^-$$
$$+ \mathbf{h}^- \cdot \mathbf{m}^+ - \mathbf{e}^+ \cdot \mathbf{j}^- + R^{-1}\, h^{-1}(h_y^-\, e_\zeta^+ + e_y^+\, h_\zeta^-) = -2jk_\zeta\, h^{-1}\left(\mathbf{e}_t^+ \times \mathbf{h}_t^+\right) \cdot \mathbf{u}_\zeta.$$
$$(2\text{-}36)$$

Integrating the above over the waveguide cross-sections, after trivial rearrangement, yields:

$$k_\zeta = \frac{I_N}{I_D}, \qquad (2\text{-}37)$$

where

$$I_N = \int_S \Big[\omega\epsilon\, \mathbf{e}^+ \cdot \mathbf{e}^- - \omega\mu\, \mathbf{h}^- \cdot \mathbf{h}^+ + j\, \mathbf{h}^- \cdot \boldsymbol{\nabla}_t \times \mathbf{e}^+ + j\, \mathbf{e}^+ \cdot \boldsymbol{\nabla}_t \times \mathbf{h}^-$$
$$+ j\, \mathbf{h}^- \cdot \mathbf{m}^+ - j\, \mathbf{e}^+ \cdot \mathbf{j}^- + j\, R^{-1}\, h^{-1}(h_y^-\, e_\zeta^+ + e_y^+\, h_\zeta^-)\Big]\, ds \quad (2\text{-}38)$$

$$I_D = 2 \int_S h^{-1}\left(\mathbf{e}_t^+ \times \mathbf{h}_t^+\right) \cdot \mathbf{u}_\zeta\, ds. \qquad (2\text{-}39)$$

In the special source-free ($\mathbf{m}^+ \to \mathbf{0}$ and $\mathbf{j}^- \to \mathbf{0}$) and curvature vanishing scenario ($R^{-1} \to 0$), we have $h \to 1$, $\mathbf{u}_\zeta \to \mathbf{u}_z$, and the above -reduces to the variational formula in [1, eq. (7-86)].

$$I_N = \int_S \Big[\omega\epsilon\, \mathbf{e}^+ \cdot \mathbf{e}^- - \omega\mu\, \mathbf{h}^- \cdot \mathbf{h}^+ + j\, \mathbf{h}^- \cdot \boldsymbol{\nabla}_t \times \mathbf{e}^+ + j\, \mathbf{e}^+ \cdot \boldsymbol{\nabla}_t \times \mathbf{h}^-\Big]\, ds$$
$$(2\text{-}40)$$

$$I_D = 2 \int_S \left(\mathbf{e}_t^+ \times \mathbf{h}_t^+\right) \cdot \mathbf{u}_z\, ds. \qquad (2\text{-}41)$$

2.2
A Rayleigh-Ritz Solution

Let us define the field expansion as

$$\mathbf{e}^+ = \sum_{i=1}^{N} \mathbf{e}_i(\rho, \phi)\, a_i^e = \bar{E}^T\, \bar{A}^e = \bar{A}^{eT}\, \bar{E} \tag{2-42}$$

$$\mathbf{h}^+ = \sum_{i=1}^{N} \mathbf{h}_i(\rho, \phi)\, a_i^h = \bar{H}^T\, \bar{A}^h = \bar{A}^{hT}\, \bar{H}. \tag{2-43}$$

where the harmonics fields of the expansion, e_i or h_i, can be written in system of a vectors $\bar{E}$ or $\bar{H}$ and a_i^e and a_i^h are variational parameters, that can be conveniently arranged into an unknown vector $\bar{A}$. We can use the mirror-mode symmetric relation for obtaining $\mathbf{e}^-$ and $\mathbf{h}^-$ via (2-3). In the above, the superscript T refers to a transpose of a vector.

Accordingly, all terms of the equation (2-40) and (2-41) can be written in a matrix form as

$$I_N = \bar{A}^T \bar{\bar{N}} \bar{A}, \tag{2-44}$$

$$I_D = \bar{A}^T \bar{\bar{D}} \bar{A}. \tag{2-45}$$

Now we have defined the constant matrices $\bar{\bar{N}}$ and $\bar{\bar{D}}$, the longitudinal wavenumber formula in (2-37) can be written as

$$k_\zeta = (\bar{A}^T \bar{\bar{D}} \bar{A})^{-1} (\bar{A}^T \bar{\bar{N}} \bar{A}). \tag{2-46}$$

Next, the stationary conditions

$$\frac{\partial}{\partial A_i} k_\zeta = 0, \quad \text{for} \quad i = \{1, 2, 3, \ldots, N\} \tag{2-47}$$

will provide the best approximations for $\bar{A}$. Accordingly, we must enforce

$$\frac{I_D I_N' - I_N I_D'}{I_D^2} = 0, \quad \text{for} \quad i = \{1, 2, 3, \ldots, N\}. \tag{2-48}$$

where the prime ($'$) represents $\partial/\partial A_i$. Assuming that I_D^2 is free of singularities, we have to solve the system of equations

$$I_D I_N' - I_N I_D' = 0, \quad \text{for} \quad i = \{1, 2, 3, \ldots, N\}. \tag{2-49}$$

Substituting (2-44) and (2-45) into the above, we obtain

$$\bar{A}^T\bar{\bar{D}}\bar{A}\frac{\partial}{\partial A_i}\left(\bar{A}^T\bar{\bar{N}}\bar{A}\right) - \bar{A}^T\bar{\bar{N}}\bar{A}\frac{\partial}{\partial A_i}\left(\bar{A}^T\bar{\bar{D}}\bar{A}\right) = 0, \text{ for } i = \{1,2,3,\ldots,N\}.$$

(2-50)

The above set of equations can be compactly written as the vector equation

$$\bar{A}^T\bar{\bar{D}}\bar{A}\frac{\partial}{\partial\bar{A}}\left(\bar{A}^T\bar{\bar{N}}\bar{A}\right) - \bar{A}^T\bar{\bar{N}}\bar{A}\frac{\partial}{\partial\bar{A}}\left(\bar{A}^T\bar{\bar{D}}\bar{A}\right) = \bar{0}.$$

(2-51)

Using the result [20, eq. (81)]

$$\frac{\partial}{\partial\bar{A}}\left(\bar{A}^T\bar{\bar{M}}\bar{A}\right) = (\bar{\bar{M}} + \bar{\bar{M}}^T)\bar{A},$$

(2-52)

assuming $\bar{\bar{M}} = \{\bar{\bar{N}}, \bar{\bar{D}}\}$ is a symmetric matrix with $\bar{\bar{M}} = \bar{\bar{M}}^T$, we obtain

$$\frac{\partial}{\partial\bar{A}}\left(\bar{A}^T\bar{\bar{M}}\bar{A}\right) = 2\bar{\bar{M}}\bar{A}.$$

(2-53)

Equation (2-51) then yields

$$2\bar{A}^T\bar{\bar{D}}\bar{A}\bar{\bar{N}}\bar{A} - 2\bar{A}^T\bar{\bar{N}}\bar{A}\bar{\bar{D}}\bar{A} = \bar{0}.$$

(2-54)

Next, division of the above by $2\bar{A}^T\bar{\bar{D}}\bar{A}$ yields

$$\bar{\bar{N}}\bar{A} - (\bar{A}^T\bar{\bar{D}}\bar{A})^{-1}(\bar{A}^T\bar{\bar{N}}\bar{A})\bar{\bar{D}}\bar{A} = \bar{0}.$$

(2-55)

Using (2-46), we obtain

$$\bar{\bar{N}}\bar{A} - k_\zeta\bar{\bar{D}}\bar{A} = \bar{0},$$

(2-56)

or

$$(\bar{\bar{N}} - k_\zeta\bar{\bar{D}})\bar{A} = \bar{0},$$

(2-57)

3
H-plane Bend Rectangular Waveguide

3.1
Theory

In the case of a rectangular waveguide depicted in Fig. 3.1, a TE^ζ mode can be defined in terms of the wave potential

$$\psi_{mn}^{\text{TE}}(x, y, z) = \sum_{m=1}^{M} A_m \, \cos \frac{m\pi x}{a} \, \cos \frac{n\pi y}{b} \, e^{-jk_z z}. \qquad (3\text{-}1)$$

The fundamental mode in an straight $(R \to \infty)$ waveguide with $a > b$ has a TE_{10}^z field with $m = 1$ and $n = 0$, i.e., $\partial/\partial y = 0$ is main configuration of interest. For a finite R, our fields will also have $\partial/\partial y = 0$, and will be associated with the modal index $n = 0$.

According to [1, eq. (3-89)], e_x, e_ζ and h_y will be null and as $n = 0$, the field component e_y is the only non-null electric field inside the waveguide [21, p. 366]. Accordingly, we express the modal electric field via

$$e_y^{TE} = \frac{\partial \psi}{\partial x} = \sum_{m=1}^{M} -A_m \, \frac{m\pi}{a} \, \sin \frac{m\pi x}{a}. \qquad (3\text{-}2)$$

By using the relations in [22, p. 50], in a toroidal coordinate system we
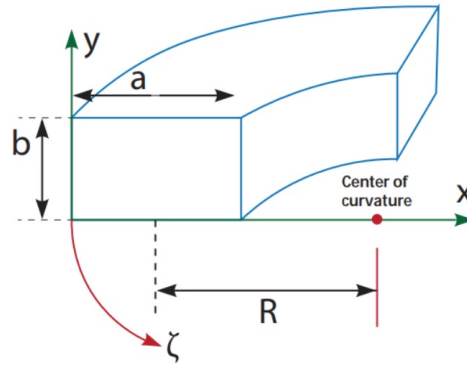
Figure 3.1: H-plane bend rectangular waveguide.

have to satisfy

$$\frac{\partial e_z}{\partial y} - \frac{\partial e_y}{\partial \zeta} = -j\omega\mu\, h\, h_x, \tag{3-3}$$

where h is the metric component for the ζ-direction adapted to the problem in Fig. 3.1, i.e., $h = 1 - R^{-1}(x - a/2)$.

We can express the x-component of the magnetic field via

$$h_x = (j\omega\mu)^{-1}\, h^{-1}\, \frac{\partial e_y}{\partial \zeta} \tag{3-4}$$

$$= (j\omega\mu)^{-1}\, h^{-1}\, (-jk_\zeta) e_y \tag{3-5}$$

$$= (j\omega\mu)^{-1}\, h^{-1}\, (-jk_\zeta) \sum_{m=1}^{M} -A_m\, \frac{m\pi}{a}\, \sin\frac{m\pi x}{a} \tag{3-6}$$

$$= (\omega\mu)^{-1} \sum_{m=1}^{M} A_m\, h^{-1}\, k_\zeta\, \frac{m\pi}{a}\, \sin\frac{m\pi x}{a}. \tag{3-7}$$

An important point to note is that the presence of k_ζ in h_x, that is a direct result of the partial derivative with respect to ζ, which should be taken into consideration in (2-37).

Using the relations below for h_ζ in the formulas in [22, p. 50], we can write

$$\frac{\partial e_y}{\partial x} - \frac{\partial e_x}{\partial y} = -j\omega\mu\, h_\zeta, \tag{3-8}$$

where h_ζ can be written as

$$h_\zeta = (-j\omega\mu)^{-1}\, \frac{\partial e_y}{\partial x} \tag{3-9}$$

$$= (j\omega\mu)^{-1} \sum_{m=1}^{M} A_m \left(\frac{m\pi}{a}\right)^2 \cos\frac{m\pi x}{a}. \tag{3-10}$$

Let us now use the above into our variational formula in (2-37). The first term of I_N in (2-40) will be denoted here as I_{N1}:

$$I_{N1} = \int_S \left(\omega\epsilon\, \mathbf{e}^+ \cdot \mathbf{e}^-\right) ds, \tag{3-11}$$

that can be expressed as

$$I_{N1} = \int_S \omega\epsilon \left(\mathbf{e}_t + e_\zeta\right) \cdot \left(\mathbf{e}_t - e_\zeta\right) ds \tag{3-12}$$

$$= \int_S \omega\epsilon \left(e_x\,e_x + e_y\,e_y\right) - e_\zeta\,e_\zeta\,ds. \tag{3-13}$$

Since e_x and e_ζ are null, the above can be written as

$$I_{N1} = b\omega\epsilon \int_{x=0}^a e_y\,e_y\,dx. \tag{3-14}$$

Additionally, we can be write

$$I_{N1} = \int_{x=0}^a \bar{A}^T \bar{e}_y \bar{e}_y^{\ T} \bar{A}\,dx, \tag{3-15}$$

or

$$I_{N1} = \bar{A}^T \bar{\bar{N}}_1 \bar{A}, \tag{3-16}$$

where we have introduced the matrix $\bar{\bar{N}}$, filled according to

$$\bar{\bar{N}}_1|_{m,m'} = b\omega\epsilon \int_{x=0}^a e_{y,m}\,e_{y,m'}\,dx \tag{3-17}$$

$$= b\omega\epsilon \int_{x=0}^a \left[\frac{m\pi}{a}\,\sin\frac{m\pi x}{a}\right] \cdot \left[\frac{m'\pi}{a}\,\sin\frac{m'\pi x}{a}\right] dx. \tag{3-18}$$

The modal amplitudes A_m were arranged in the column vector $\bar{A}$.

The second term in I_N will be denoted as I_{N2}, such as

$$I_{N2} = \int_S -\left(\omega\mu\,\mathbf{h}^- \cdot \mathbf{h}^+\right) ds. \tag{3-19}$$

As this mode do not have h_y, the above can be written as

$$I_{N2} = \int_S -\omega\mu \left[-\left(\mathbf{u}_x h_x + \mathbf{u}_y h_y\right) + \mathbf{u}_\zeta h_\zeta \cdot \left(\mathbf{u}_x h_x + \mathbf{u}_y h_y\right) + \mathbf{u}_\zeta h_\zeta\right] ds \tag{3-20}$$

$$= \int_S -\omega\mu \left[\left(-\mathbf{u}_x h_x + \mathbf{u}_\zeta h_\zeta\right) \cdot \left(\mathbf{u}_x h_x + \mathbf{u}_\zeta h_\zeta\right)\right] ds \tag{3-21}$$

$$= -\omega\mu \int_S \left[-\left(h_x h_x\right) + \left(h_\zeta h_\zeta\right)\right] ds \tag{3-22}$$

$$= -b\omega\mu \int_{x=0}^a \left[-\left(h_x h_x\right) + \left(h_\zeta h_\zeta\right)\right] dx. \tag{3-23}$$

Moreover, the above can be rewritten as

$$I_{N2} = -b\omega\mu \int_{x=0}^a \left(-\bar{A}^T \bar{h}_x \bar{h}_x^{\ T} \bar{A} + \bar{A}^T \bar{h}_\zeta \bar{h}_\zeta^{\ T} \bar{A}\right) dx \tag{3-24}$$

and finally

$$I_{N2} = \bar{A}^T \bar{\bar{N}}_{21} \bar{A} + \bar{A}^T \bar{\bar{N}}_{22} \bar{A}. \tag{3-25}$$

In the above, we introduced the matrix $\bar{\bar{N}}_{21}$, such as

$$\bar{\bar{N}}_{21}|_{m,m'} = b\omega\mu \int_{x=0}^{a} h_{x,m} \, h_{x,m'} \, dx \tag{3-26}$$

$$= b\omega\mu \int_{x=0}^{a} \left[(\omega\mu)^{-1} h^{-1} k_\zeta \, \frac{m\pi}{a} \, \sin\frac{m\pi x}{a} \right]$$

$$\cdot \left[(\omega\mu)^{-1} h^{-1} k_\zeta \, \frac{m'\pi}{a} \, \sin\frac{m'\pi x}{a} \right] dx. \tag{3-27}$$

Notice that in $\bar{\bar{N}}_{21}$ have appeared a term proportional to k_ζ^2. The other matrix constituent of I_{N2} in (3-25) is given by

$$\bar{\bar{N}}_{22}|_{m,m'} = -b\omega\mu \int_{x=0}^{a} h_{\zeta,m} \, h_{\zeta,m'} \, dx \tag{3-28}$$

$$= -b\omega\mu \int_{x=0}^{a} \left[(j\omega\mu)^{-1} (\frac{m\pi}{a})^2 \, \cos\frac{m\pi x}{a} \right]$$

$$\cdot \left[(j\omega\mu)^{-1} (\frac{m'\pi}{a})^2 \, \cos\frac{m'\pi x}{a} \right] dx. \tag{3-29}$$

The third term of I_N in (2-40) is denoted here as I_{N3}, and is given by

$$I_{N3} = \int_S +j \, \mathbf{h}^- \cdot \boldsymbol{\nabla}_t \times \mathbf{e}^+ \, ds, \tag{3-30}$$

where the transversal nabla is given by

$$\boldsymbol{\nabla}_t = \mathbf{u}_x \frac{\partial}{\partial x} + \mathbf{u}_y \frac{\partial}{\partial y}. \tag{3-31}$$

Since $\partial/\partial y = 0$ and h_y, e_ζ and e_x are null, the above can by further simplified:

$$I_{N3} = \int_S +j \, \mathbf{h}^- \cdot \mathbf{u}_x \frac{\partial}{\partial x} \times \mathbf{u}_y \, e_y \, ds \tag{3-32}$$

$$= \int_S +j \, \mathbf{h}^- \cdot \mathbf{u}_\zeta \frac{\partial}{\partial x} e_y \, ds \tag{3-33}$$

$$= \int_S +j \left[-(\mathbf{u}_x h_x + \mathbf{u}_y h_y) + \mathbf{u}_\zeta h_\zeta \right] \cdot \mathbf{u}_\zeta \frac{\partial}{\partial x} e_y \, ds \tag{3-34}$$

$$= \int_S +j \, \mathbf{u}_\zeta h_\zeta \cdot \mathbf{u}_\zeta \frac{\partial}{\partial x} e_y \, ds \tag{3-35}$$

$$= \int_S +j \, h_\zeta \frac{\partial}{\partial x} e_y \, ds \tag{3-36}$$

$$= jb \int_{x=0}^{a} h_\zeta \frac{\partial}{\partial x} e_y \, dx. \tag{3-37}$$

In the vector form, the above becomes

$$I_{N3} = jb \int_{x=0}^{a} \bar{A}^T \bar{h}_\zeta \frac{\partial}{\partial x} \bar{e}_y^T \bar{A} \, dx. \tag{3-38}$$

By introducing the matrix $\bar{\bar{N}}_3$, we have

$$I_{N3} = \bar{A}^T \bar{\bar{N}}_3 \bar{A} \tag{3-39}$$

where

$$\bar{\bar{N}}_3|_{m,m'} = jb \int_{x=0}^{a} h_{\zeta,m} \frac{\partial}{\partial x} e_{y,m'} \, dx \tag{3-40}$$

$$= jb \int_{x=0}^{a} \left[(j\omega\mu)^{-1} (\frac{m\pi}{a})^2 \cos \frac{m\pi x}{a} \right]$$

$$\cdot \frac{\partial \left[-\frac{m'\pi}{a} \sin \frac{m'\pi x}{a} \right]}{\partial x} \, dx \tag{3-41}$$

$$= jb \int_{x=0}^{a} \left[(j\omega\mu)^{-1} \left(\frac{m\pi}{a} \right)^2 \cos \frac{m\pi x}{a} \right]$$

$$\cdot \left[-\left(\frac{m'\pi}{a} \right)^2 \cos \frac{m'\pi x}{a} \right] \, dx. \tag{3-42}$$

The fourth term of I_N in (2-40) was defined as

$$I_{N4} = \int_{S} +j \, \mathbf{e}^+ \cdot \boldsymbol{\nabla}_t \times \mathbf{h}^- \, ds. \tag{3-43}$$

The above can be written as

$$I_{N4} = j \int_{S} \mathbf{u}_y e_y \cdot \left[\mathbf{u}_x \frac{\partial}{\partial x} \times (-\mathbf{u}_x h_x + \mathbf{u}_\zeta h_\zeta) \right] ds \tag{3-44}$$

$$I_{N4} = j \int_{S} \mathbf{u}_y e_y \cdot \left(-\mathbf{u}_y \frac{\partial}{\partial x} h_\zeta \right) ds \tag{3-45}$$

$$I_{N4} = j \int_{S} -e_y \frac{\partial}{\partial x} h_\zeta \, ds \tag{3-46}$$

$$I_{N4} = -jb \int_{x=0}^{a} e_y \frac{\partial}{\partial x} h_\zeta \, dx. \tag{3-47}$$

In the vector form, we have

$$I_{N4} = -jb \int_{x=0}^{a} \bar{A}^T \bar{e}_y \frac{\partial}{\partial x} \bar{h}_\zeta^T \bar{A} \, dx. \tag{3-48}$$

By introducing the matrix $\bar{\bar{N}}_4$, we have

$$I_{N4} = \bar{A}^T \bar{\bar{N}}_4 \bar{A} \tag{3-49}$$

where

$$\bar{\bar{N}}_4|_{m,m'} = -jb \int_{x=0}^{a} e_{y,m} \frac{\partial}{\partial x} h_{\zeta,m'} \, dx \tag{3-50}$$

$$= -jb \int_{x=0}^{a} \left[-\frac{m\pi}{a} \sin \frac{m\pi x}{a} \right] \cdot \frac{\partial \left[(j\omega\mu)^{-1} \left(\frac{m'\pi}{a} \right)^2 \cos \frac{m'\pi x}{a} \right]}{\partial x} \, dx \tag{3-51}$$

$$= -jb \int_{x=0}^{a} \left[\frac{m\pi}{a} \sin \frac{m\pi x}{a} \right] \cdot \left[(j\omega\mu)^{-1} \left(\frac{m'\pi}{a} \right)^3 \sin \frac{m'\pi x}{a} \right] \, dx. \tag{3-52}$$

The fifth term of I_N in (2-40) can be defined as

$$I_{N5} = \int_S +R^{-1} \, h^{-1} (h_y^- \, e_\zeta^+ + e_y^+ \, h_\zeta^-) \, ds. \tag{3-53}$$

In the TE^ζ mode, the above becomes

$$I_{N5} = \int_S +jR^{-1} \, h^{-1} (e_y^+ \, h_\zeta^-) \, ds, \tag{3-54}$$

and as h_ζ^- by the mirror-mode symmetric relation is equal to h_ζ^+, we have

$$I_{N5} = +j \int_S R^{-1} \, h^{-1} (e_y \, h_\zeta) \, ds \tag{3-55}$$

$$= +jb \int_{x=0}^{a} R^{-1} \, h^{-1} (e_y \, h_\zeta) \, dx \tag{3-56}$$

In the vector form, we can write

$$I_{N5} = +jb \int_{x=0}^{a} R^{-1} \, h^{-1} \, h^{-1} \bar{A}^T \bar{e}_y \bar{h}_\zeta^{\,T} \bar{A} \, dx, \tag{3-57}$$

or

$$I_{N5} = \bar{A}^T \bar{\bar{N}}_5 \bar{A}, \tag{3-58}$$

where we have introduced the matrix $\bar{\bar{N}}_5$ via

$$\bar{\bar{N}}_5|_{m,m'} = +jb \int_{x=0}^{a} R^{-1} \, h^{-1} e_{y,m} \, h_{\zeta,m'} \, dx \tag{3-59}$$

$$= +jb \int_{x=0}^{a} R^{-1} \, h^{-1} \left[-\frac{m\pi}{a} \sin \frac{m\pi x}{a} \right]$$

$$\cdot \left[(j\omega\mu)^{-1} \left(\frac{m'\pi}{a} \right)^2 \cos \frac{m'\pi x}{a} \right] \, dx. \tag{3-60}$$

The denominator I_D in (2-37) can be written as

$$I_D = 2 \int_S h^{-1} \, (\mathbf{e}_t^+ \times \mathbf{h}_t^+) \cdot \mathbf{u}_\zeta \, ds \tag{3-61}$$

$$= 2 \int_S h^{-1} \left[(\mathbf{u}_x e_x + \mathbf{u}_y e_y) \times (\mathbf{u}_x h_x + \mathbf{u}_y h_y) \right] \cdot \mathbf{u}_\zeta \, ds \tag{3-62}$$

$$= 2 \int_S h^{-1} \left(\mathbf{u}_y e_y \times \mathbf{u}_x h_x \right) \cdot \mathbf{u}_\zeta \, ds \tag{3-63}$$

$$= 2 \int_S h^{-1} \left(-\mathbf{u}_\zeta e_y \, h_x \right) \cdot \mathbf{u}_\zeta \, ds \tag{3-64}$$

$$= -2 \int_S h^{-1} e_y \, h_x \, ds \tag{3-65}$$

$$= -2b \int_{x=0}^a h^{-1} e_y \, h_x \, dx. \tag{3-66}$$

In the vector form, the above becomes

$$I_D = -2b \int_{x=0}^a h^{-1} \bar{A}^T \bar{e}_y \bar{h}_x^{\;T} \bar{A} \, dx, \tag{3-67}$$

or

$$I_D = \bar{A}^T \bar{\bar{D}} \bar{A}, \tag{3-68}$$

where the matrix $\bar{\bar{D}}$ is given by

$$\bar{\bar{D}}|_{m,m'} = -2b \int_{x=0}^a h^{-1} e_{y,m} \, h_{x,m'} \, dx \tag{3-69}$$

$$= -2b \int_{x=0}^a h^{-1} \left[-\frac{m\pi}{a} \sin\left(\frac{m\pi x}{a}\right) \right]$$
$$\times \left[(\omega\mu)^{-1} h^{-1} k_\zeta \frac{m'\pi}{a} \sin\left(\frac{m'\pi x}{a}\right) \right] \, dx \tag{3-70}$$

Notice that we have a term proportional to k_ζ in $\bar{\bar{D}}$ and to k_ζ^2 in the matrix $\bar{\bar{N}}_{21}$. In view of obtaining a linear eigenvalue problem, we can express (2-37) in the shape of (2-46) via

$$k_\zeta^2 \bar{A}^T \bar{\bar{\bar{D}}} \bar{A} = \bar{A}^T \bar{\bar{\bar{N}}} \bar{A}. \tag{3-71}$$

where

$$\bar{\bar{\bar{N}}} = \bar{\bar{N}}_1 + \bar{\bar{N}}_{22} + \bar{\bar{N}}_3 + \bar{\bar{N}}_4 + \bar{\bar{N}}_5, \tag{3-72}$$

$$\bar{\bar{\bar{D}}} = k_\zeta^{-1} \bar{\bar{D}} - k_\zeta^{-2} \bar{\bar{N}}_{21}. \tag{3-73}$$

We can now impose the stationary conditions into (3-71), resulting in

$$\frac{\partial}{\partial \bar{A}} \left[\bar{A}^T \left(k_\zeta^2 \bar{\bar{\bar{D}}} - \bar{\bar{\bar{N}}} \right) \bar{A} \right] = \bar{0}. \tag{3-74}$$

The above renders

$$k_\zeta^2 \left(\frac{\bar{\bar{\tilde{D}}} + \bar{\bar{\tilde{D}}}^T}{2} \right) \bar{A} - \left(\frac{\bar{\bar{\tilde{N}}} + \bar{\bar{\tilde{N}}}^T}{2} \right) \bar{A} = \bar{0}. \qquad (3\text{-}75)$$

Introducing the double-tild matrices

$$\bar{\bar{\tilde{\tilde{N}}}} = \frac{\bar{\bar{\tilde{N}}} + \bar{\bar{\tilde{N}}}^T}{2}, \qquad (3\text{-}76)$$

$$\bar{\bar{\tilde{\tilde{D}}}} = \frac{\bar{\bar{\tilde{D}}} + \bar{\bar{\tilde{D}}}^T}{2}, \qquad (3\text{-}77)$$

$$(3\text{-}78)$$

we obtain the linear eigenvalue problem

$$\left(k_\zeta^2 \bar{\bar{\tilde{\tilde{D}}}} - \bar{\bar{\tilde{\tilde{N}}}} \right) \bar{A} = \bar{0}. \qquad (3\text{-}79)$$

We have used the Matlab framework [23] to solve the generalized eigenvalue problem in (3-79) via the command

```
[mat_V, mat_L] = eig( mat_tilde_tilde_N, mat_tilde_tilde_D );
```

Note that `mat_L` is a diagonal matrix with the eigenvalues of the problem, that allows us to obtain the longitudinal wavenumbers k_ζ via the command

```
k_zeta = sqrt( diag(mat_L));
```

The associated eigenvectors $\bar{A}$ (for all of the found k_ζ) are assembled into the columns of the computational matrix `mat_V`.

3.2
Numerical Results

3.2.1
H-plane bend waveguide with $R/a = 0.75$

We first consider an H-plane bend waveguide with $a = 22.86$ mm and $b = 10.16$ mm, operating at 10 GHz and with radius R/a as depicted in Fig. 3.2.

The first 10 normalized longitudinal wavenumbers for TE_{m0}^ζ modes obtained by our method with $R/a = 0.75$ are shown in Tables 3.1–3.4. Our method were compared against the exact (reference) [12] and perturbation [2] solutions. Perturbational methods involve solving a problem by making a small change, or perturbation, to an existing solution or model and assumes that the
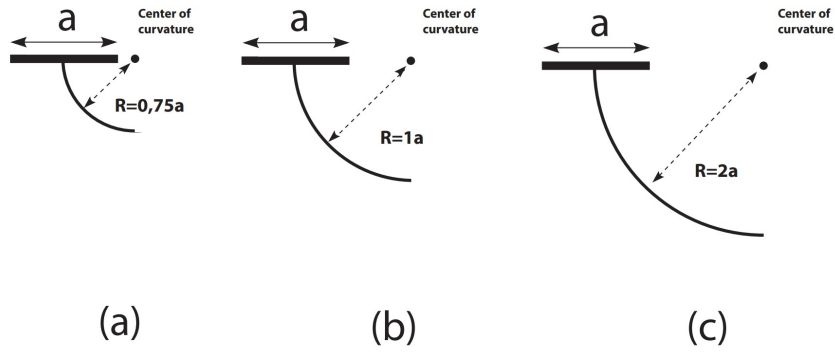
Figure 3.2: Radius of a curved waveguide (a) $R/a = 0.75$, (b) $R/a = 1$ and (c) $R/a = 2$.

problem can be simplified by analyzing the effects of small deviations from a known solution. The approximated longitudinal wavenumbers are denoted as k_ζ, and we evaluate the convergence as $M = \{10, 15, 20\}$. The results obtained via the present variational method show good agreement. Note that the relative error observed in the first modes in the perturbational results are generally larger than the ones observed in our method. The error of the perturbational approach in Table 3.1 becomes asymptotically close to 1.2%. This is due to the methods in [2] being limited up to $\mathcal{O}(R^{-2})$ correction.

Table 3.1: Normalized longitudinal wavenumbers k_ζ/k for TE$^\zeta$ modes in an H-plane bend waveguide (with $R/a = 0.75$) obtained by the exact (reference) solution [12] and the perturbation solution [2].

Mode	Ref. [12]	Perturbation Ref. [2]	Rel. error (%)
TE$^\zeta_{10}$	7.4023e-01	7.4045e-01	2.9991e-02
TE$^\zeta_{20}$	$-j\,6.7168$e-01	$-j\,6.7591$e-01	6.2892e-01
TE$^\zeta_{30}$	$-j\,1.3716$e+00	$-j\,1.3867$e+00	1.1072e+00
TE$^\zeta_{40}$	$-j\,1.9816$e+00	$-j\,2.0050$e+00	1.1822e+00
TE$^\zeta_{50}$	$-j\,2.5635$e+00	$-j\,2.5947$e+00	1.2162e+00
TE$^\zeta_{60}$	$-j\,3.1323$e+00	$-j\,3.1709$e+00	1.2329e+00
TE$^\zeta_{70}$	$-j\,3.6937$e+00	$-j\,3.7396$e+00	1.2417e+00
TE$^\zeta_{80}$	$-j\,4.2505$e+00	$-j\,4.3035$e+00	1.2468e+00
TE$^\zeta_{90}$	$-j\,4.8043$e+00	$-j\,4.8644$e+00	1.2499e+00
TE$^\zeta_{10,0}$	$-j\,5.3560$e+00	$-j\,5.4231$e+00	1.2520e+00

Table 3.2: Normalized longitudinal wavenumbers k_ζ/k for TE^ζ modes in an H-plane bend waveguide (with $R/a = 0.75$) obtained by the exact (reference) solution [12] and our method with $M = 10$.

Mode	Ref. [12]	Our method with $M = 10$	Rel. error (%)
TE_{10}^ζ	7.4023e-01	7.4023e-01	5.6351e-05
TE_{20}^ζ	$-j\,6.7168$e-01	$-j\,6.7170$e-01	1.8381e-03
TE_{30}^ζ	$-j\,1.3716$e+00	$-j\,1.3721$e+00	3.7460e-02
TE_{40}^ζ	$-j\,1.9816$e+00	$-j\,1.9871$e+00	2.8132e-01
TE_{50}^ζ	$-j\,2.5635$e+00	$-j\,2.5964$e+00	1.2827e+00
TE_{60}^ζ	$-j\,3.1323$e+00	$-j\,3.2548$e+00	3.9120e+00
TE_{70}^ζ	$-j\,3.6937$e+00	$-j\,4.0174$e+00	8.7635e+00
TE_{80}^ζ	$-j\,4.2505$e+00	$-j\,4.9480$e+00	1.6409e+01
TE_{90}^ζ	$-j\,4.8043$e+00	$-j\,6.1413$e+00	2.7829e+01
$TE_{10,0}^\zeta$	$-j\,5.3560$e+00	$-j\,7.9690$e+00	4.8785e+01

Table 3.3: Normalized longitudinal wavenumbers k_ζ/k for TE^ζ modes in an H-plane bend waveguide (with $R/a = 0.75$) obtained by the exact (reference) solution [12] and our method with $M = 15$.

Mode	Ref. [12]	Our method with $M = 15$	Rel. error (%)
TE_{10}^ζ	7.4023e-01	7.4023e-01	5.0312e-06
TE_{20}^ζ	$-j\,6.7168$e-01	$-j\,6.7168$e-01	1.3177e-04
TE_{30}^ζ	$-j\,1.3716$e+00	$-j\,1.3716$e+00	2.2378e-03
TE_{40}^ζ	$-j\,1.9816$e+00	$-j\,1.9818$e+00	1.4713e-02
TE_{50}^ζ	$-j\,2.5635$e+00	$-j\,2.5654$e+00	7.1858e-02
TE_{60}^ζ	$-j\,3.1323$e+00	$-j\,3.1412$e+00	2.8389e-01
TE_{70}^ζ	$-j\,3.6937$e+00	$-j\,3.7269$e+00	8.9950e-01
TE_{80}^ζ	$-j\,4.2505$e+00	$-j\,4.3459$e+00	2.2447e+00
TE_{90}^ζ	$-j\,4.8043$e+00	$-j\,5.0236$e+00	4.5647e+00
$TE_{10,0}^\zeta$	$-j\,5.3560$e+00	$-j\,5.7820$e+00	7.9537e+00
$TE_{11,0}^\zeta$	$-j\,5.9062$e+00	$-j\,6.6471$e+00	1.2544e+01
$TE_{12,0}^\zeta$	$-j\,6.4552$e+00	$-j\,7.6505$e+00	1.8518e+01
$TE_{13,0}^\zeta$	$-j\,7.0033$e+00	$-j\,8.8604$e+00	2.6517e+01

Table 3.4: Normalized longitudinal wavenumbers k_ζ/k for TE$^\zeta$ modes in an H-plane bend waveguide (with $R/a = 0.75$) obtained by the exact (reference) solution [12] and our method with $M = 20$.

Mode	Ref. [12]	Our method with $M = 20$	Rel. error (%)
TE$_{10}^\zeta$	$7.4023\text{e-}01$	$7.4023\text{e-}01$	$7.8912\text{e-}07$
TE$_{20}^\zeta$	$-j\,6.7168\text{e-}01$	$-j\,6.7168\text{e-}01$	$1.9312\text{e-}05$
TE$_{30}^\zeta$	$-j\,1.3716\text{e+}00$	$-j\,1.3716\text{e+}00$	$2.8661\text{e-}04$
TE$_{40}^\zeta$	$-j\,1.9816\text{e+}00$	$-j\,1.9816\text{e+}00$	$1.6195\text{e-}03$
TE$_{50}^\zeta$	$-j\,2.5635\text{e+}00$	$-j\,2.5637\text{e+}00$	$6.8354\text{e-}03$
TE$_{60}^\zeta$	$-j\,3.1323\text{e+}00$	$-j\,3.1331\text{e+}00$	$2.5443\text{e-}02$
TE$_{70}^\zeta$	$-j\,3.6937\text{e+}00$	$-j\,3.6969\text{e+}00$	$8.6075\text{e-}02$
TE$_{80}^\zeta$	$-j\,4.2505\text{e+}00$	$-j\,4.2616\text{e+}00$	$2.6149\text{e-}01$
TE$_{90}^\zeta$	$-j\,4.8043\text{e+}00$	$-j\,4.8373\text{e+}00$	$6.8624\text{e-}01$
TE$_{10,0}^\zeta$	$-j\,5.3560\text{e+}00$	$-j\,5.4379\text{e+}00$	$1.5290\text{e+}00$
TE$_{11,0}^\zeta$	$-j\,5.9062\text{e+}00$	$-j\,6.0782\text{e+}00$	$2.9132\text{e+}00$
TE$_{12,0}^\zeta$	$-j\,6.4552\text{e+}00$	$-j\,6.7715\text{e+}00$	$4.8999\text{e+}00$
TE$_{13,0}^\zeta$	$-j\,7.0033\text{e+}00$	$-j\,7.5288\text{e+}00$	$7.5043\text{e+}00$

In order to verify the convergence characteristics of the presented variational formulation, Fig. 3.6 and Fig. 3.7 show the relative error on the longitudinal wavenumber of TE_{10}^{ζ} and TE_{20}^{ζ} ($R/a = 0.75$) as a function of the number of harmonics M. The analytical solution from [12] was used as a reference, where the computation are presented in a 10-digit double-precision, i.e., the eigenvalues may present a relative error of 10^{-10} or less. We observe that using $M = 60$ harmonics in our formulation the relative error is smaller than 10^{-10}, proving the accuracy and the convergence of our method. As a reference for the computational cost, the CPU time required by our Matlab code (running on a regular laptop) to calculate M longitudinal wavenumbers is presented in Fig. 3.8.
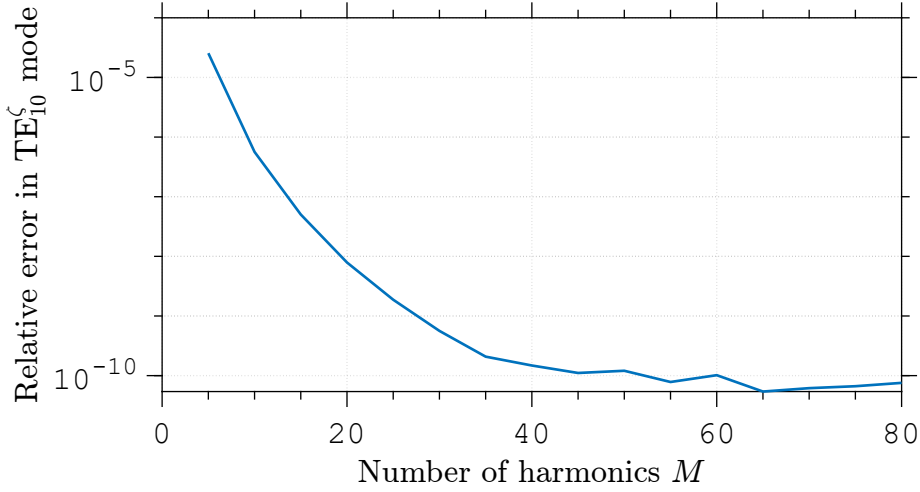

Figure 3.3: Relative error on the longitudinal wavenumber of TE_{10}^{ζ} as a function of the number of harmonics M.

Figure 3.4: Relative error on the longitudinal wavenumber of TE_{20}^{ζ} as a function of the number of harmonics M.
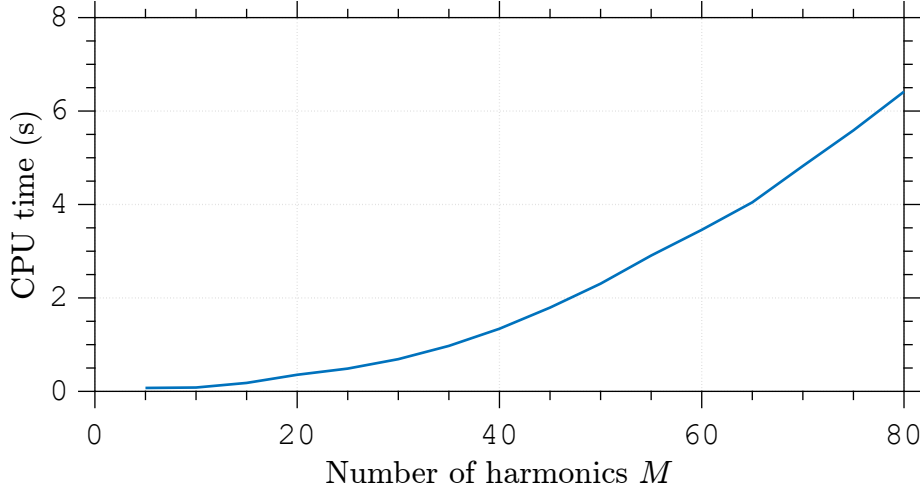
Figure 3.5: CPU time for computing M longitudinal wavenumbers.

3.2.2
H-plane bend waveguide with $R/a = 1$

Now we consider an H-plane bend waveguide with $a = 22.86$ mm and $b = 10.16$ mm, operating at 10 GHz. The first 10 normalized longitudinal wavenumbers for TE^ζ_{m0} modes obtained by our method with $R/a = 1$ are shown in Tables 3.5 and 3.6. Our method (with $M = 15$) were compared against the exact (reference) [12] and perturbation [2] solutions. The approximated longitudinal wavenumbers are denoted as k_ζ. The results obtained via the present variational method again show good agreement.

Table 3.5: Normalized longitudinal wavenumbers k_ζ/k for TE^ζ modes in an H-plane bend waveguide (with $R/a = 1$) obtained by the exact (reference) solution [12] and the perturbation solution [2].

Mode	Ref. [12]	Perturbation Ref. [2]	Rel. error (%)
TE^ζ_{10}	7.4677e-01	7.4686e-01	1.1067e-02
TE^ζ_{20}	$-j\,7.5520$e-01	$-j\,7.5625$e-01	1.3813e-01
TE^ζ_{30}	$-j\,1.5250$e+00	$-j\,1.5288$e+00	2.4900e-01
TE^ζ_{40}	$-j\,2.1926$e+00	$-j\,2.1985$e+00	2.6800e-01
TE^ζ_{50}	$-j\,2.8298$e+00	$-j\,2.8376$e+00	2.7700e-01
TE^ζ_{60}	$-j\,3.4530$e+00	$-j\,3.4627$e+00	2.8154e-01
TE^ζ_{70}	$-j\,4.0684$e+00	$-j\,4.0799$e+00	2.8402e-01
TE^ζ_{80}	$-j\,4.6791$e+00	$-j\,4.6925$e+00	2.8549e-01
TE^ζ_{90}	$-j\,5.2867$e+00	$-j\,5.3018$e+00	2.8641e-01
$\text{TE}^\zeta_{10,0}$	$-j\,5.8921$e+00	$-j\,5.9090$e+00	2.8702e-01

In order to verify the convergence characteristics of the presented variational formulation, Fig. 3.6 and Fig. 3.7 show the relative error on the longitudinal wavenumber of TE^ζ_{10} and TE^ζ_{20} as a function of the number

Table 3.6: Normalized longitudinal wavenumbers k_ζ/k for TE$^\zeta$ modes in an H-plane bend waveguide (with $R/a = 1$) obtained by the exact (reference) solution [12] and our method with $M = 15$.

Mode	Ref. [12]	Our method	Rel. error (%)
TE$_{10}^\zeta$	7.4677e-01	7.4677e-01	6.2071e-07
TE$_{20}^\zeta$	$-j\,7.5520$e-01	$-j\,7.5520$e-01	8.8741e-06
TE$_{30}^\zeta$	$-j\,1.5250$e+00	$-j\,1.5250$e+00	1.2727e-04
TE$_{40}^\zeta$	$-j\,2.1926$e+00	$-j\,2.1926$e+00	7.1067e-04
TE$_{50}^\zeta$	$-j\,2.8298$e+00	$-j\,2.8299$e+00	3.2205e-03
TE$_{60}^\zeta$	$-j\,3.4530$e+00	$-j\,3.4534$e+00	1.3152e-02
TE$_{70}^\zeta$	$-j\,4.0684$e+00	$-j\,4.0705$e+00	5.2882e-02
TE$_{80}^\zeta$	$-j\,4.6791$e+00	$-j\,4.6882$e+00	1.9530e-01
TE$_{90}^\zeta$	$-j\,5.2867$e+00	$-j\,5.3202$e+00	6.3371e-01
TE$_{10,0}^\zeta$	$-j\,5.8921$e+00	$-j\,5.9908$e+00	1.6757e+00
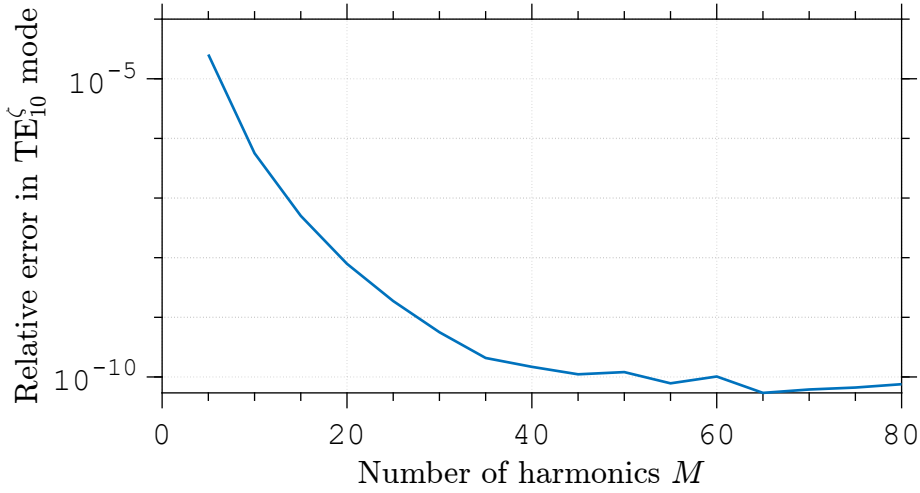
Figure 3.6: Relative error on the longitudinal wavenumber of TE$_{10}^\zeta$ as a function of the number of harmonics M.

of harmonics M. The analytical solution from [12] was used as a reference, where the computation are presented in a 10-digit double-precision, i.e., the eigenvalues may present a relative error of 10^{-10} or less. We observe that using $M = 60$ harmonics in our formulation the relative error is smaller than 10^{-10}, proving the accuracy and the convergence of our method. As a reference for the computational cost, the CPU time required by our Matlab code (running on a regular laptop) to calculate M longitudinal wavenumbers is presented in Fig. 3.8.
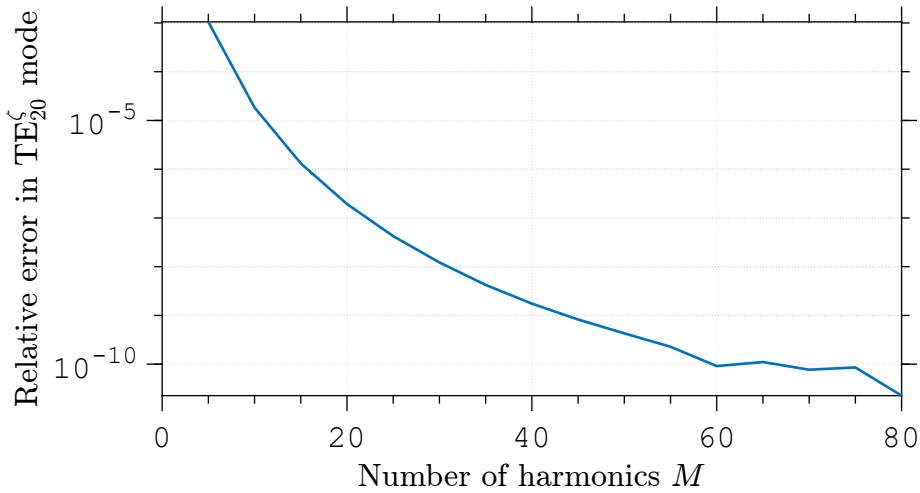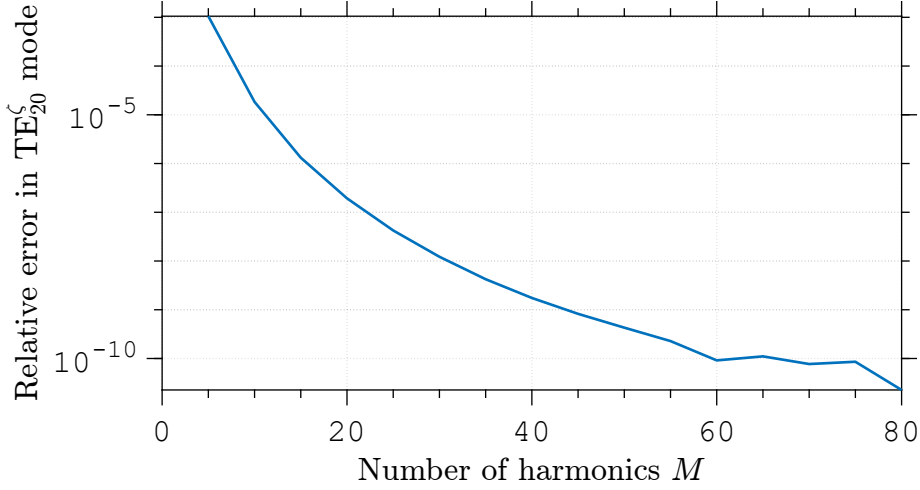
Figure 3.7: Relative error on the longitudinal wavenumber of TE_{20}^{ζ} as a function of the number of harmonics M.
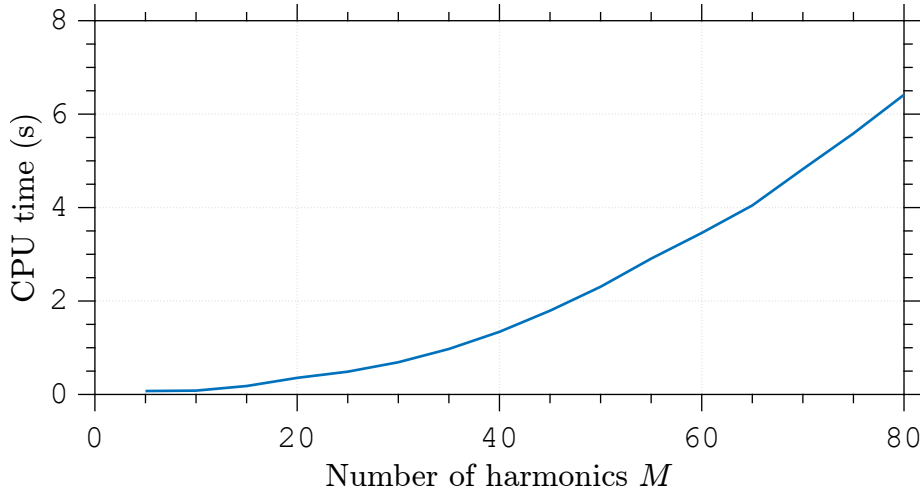
Figure 3.8: CPU time for computing M longitudinal wavenumbers.

3.2.3
H-plane bend waveguide with $R/a = 2$

Now we consider an H-plane bend waveguide with $a = 22.86$ mm and $b = 10.16$ mm, operating at 10 GHz. The first 10 normalized longitudinal wavenumbers for TE_{m0}^{ζ} modes obtained by our method with $R/a = 2$ are shown in Tables 3.7 and 3.8. Our method (with $M = 15$) were compared against the exact (reference) [12] and perturbation [2] solutions. The approximated longitudinal wavenumbers are denoted as k_ζ. The results obtained via the present variational method again show good agreement.

Table 3.7: Normalized longitudinal wavenumbers k_ζ/k for TE^ζ modes in an H-plane bend waveguide (with $R/a = 2$) obtained by the exact (reference) solution [12] and the perturbation solution [2].

Mode	Ref. [12]	Perturbation Ref. [2]	Rel. error (%)
TE_{10}^ζ	7.5297e-01	7.5298e-01	7.4979e-04
TE_{20}^ζ	$-j\,8.2630$e-01	$-j\,8.2635$e-01	6.5071e-03
TE_{30}^ζ	$-j\,1.6541$e+00	$-j\,1.6542$e+00	1.1906e-02
TE_{40}^ζ	$-j\,2.3699$e+00	$-j\,2.3702$e+00	1.2888e-02
TE_{50}^ζ	$-j\,3.0532$e+00	$-j\,3.0537$e+00	1.3365e-02
TE_{60}^ζ	$-j\,3.7219$e+00	$-j\,3.7224$e+00	1.3611e-02
TE_{70}^ζ	$-j\,4.3826$e+00	$-j\,4.3832$e+00	1.3746e-02
TE_{80}^ζ	$-j\,5.0384$e+00	$-j\,5.0391$e+00	1.3828e-02
TE_{90}^ζ	$-j\,5.6911$e+00	$-j\,5.6919$e+00	1.3880e-02
$\mathrm{TE}_{10,0}^\zeta$	$-j\,6.3415$e+00	$-j\,6.3424$e+00	1.3915e-02

Table 3.8: Normalized longitudinal wavenumbers k_ζ/k for TE^ζ modes in an H-plane bend waveguide (with $R/a = 2$) obtained by the exact (reference) solution [12] and our method with $M = 15$.

Mode	Ref. [12]	Our method	Rel. error (%)
TE_{10}^ζ	7.5297e-01	7.5297e-01	3.2882e-08
TE_{20}^ζ	$-j\,8.2630$e-01	$-j\,8.2635$e-01	2.1588e-07
TE_{30}^ζ	$-j\,1.6541$e+00	$-j\,1.6541$e+00	2.8329e-06
TE_{40}^ζ	$-j\,2.3699$e+00	$-j\,2.3699$e+00	1.1290e-05
TE_{50}^ζ	$-j\,3.0532$e+00	$-j\,3.0532$e+00	4.5240e-05
TE_{60}^ζ	$-j\,3.7219$e+00	$-j\,3.7219$e+00	1.2519e-04
TE_{70}^ζ	$-j\,4.3826$e+00	$-j\,4.3826$e+00	4.3711e-04
TE_{80}^ζ	$-j\,5.0384$e+00	$-j\,5.0385$e+00	1.2911e-03
TE_{90}^ζ	$-j\,5.6911$e+00	$-j\,5.6914$e+00	5.1057e-03
$\mathrm{TE}_{10,0}^\zeta$	$-j\,6.3415$e+00	$-j\,6.3428$e+00	1.9624e-02
$\mathrm{TE}_{11,0}^\zeta$	$-j\,6.9904$e+00	$-j\,6.9968$e+00	9.1691-02

3.2.4
H-plane bend waveguide with $R/a = 10$

Now we consider an H-plane bend waveguide with $a = 22.86$ mm and $b = 10.16$ mm, operating at 10 GHz. The first 10 normalized longitudinal wavenumbers for TE_{m0}^ζ modes obtained by our method with $R/a = 10$ are shown in Tables 3.9 and 3.10. Our method (with $M = 15$) were compared against the exact (reference) [12] and perturbation [2] solutions. The approximated longitudinal wavenumbers are denoted as k_ζ. The results obtained via the present variational method again show good agreement.

Table 3.9: Normalized longitudinal wavenumbers k_ζ/k for TE$^\zeta$ modes in an H-plane bend waveguide (with $R/a = 10$) obtained by the exact (reference) solution [12] and the perturbation solution [2].

Mode	Ref. [12]	Perturbation Ref. [2]	Rel. error (%)
TE$^\zeta_{10}$	7.5493e-01	7.5493e-01	1.2208e-06
TE$^\zeta_{20}$	$-j\,8.4756$e-01	$-j\,8.4756$e-01	9.6088e-06
TE$^\zeta_{30}$	$-j\,1.6924$e+00	$-j\,1.6924$e+00	1.7645e-05
TE$^\zeta_{40}$	$-j\,2.4226$e+00	$-j\,2.4226$e+00	1.9130e-05
TE$^\zeta_{50}$	$-j\,3.1196$e+00	$-j\,3.1196$e+00	1.9858e-05
TE$^\zeta_{60}$	$-j\,3.8018$e+00	$-j\,3.8018$e+00	2.0233e-05
TE$^\zeta_{70}$	$-j\,4.4759$e+00	$-j\,4.4759$e+00	2.0441e-05
TE$^\zeta_{80}$	$-j\,5.1451$e+00	$-j\,5.1451$e+00	2.0566e-05
TE$^\zeta_{90}$	$-j\,5.8112$e+00	$-j\,5.8112$e+00	2.0646e-05
TE$^\zeta_{10,0}$	$-j\,6.4750$e+00	$-j\,6.4750$e+00	2.0700e-05

Table 3.10: Normalized longitudinal wavenumbers k_ζ/k for TE$^\zeta$ modes in an H-plane bend waveguide (with $R/a = 10$) obtained by the exact (reference) solution [12] and our method with $M = 15$.

Mode	Ref. [12]	Our method	Rel. error (%)
TE$^\zeta_{10}$	7.5493e-01	7.5493e-01	7.3883e-10
TE$^\zeta_{20}$	$-j\,8.4756$e-01	$-j\,8.4756$e-01	2.5738e-09
TE$^\zeta_{30}$	$-j\,1.6924$e+00	$-j\,1.6924$e+00	3.9058e-08
TE$^\zeta_{40}$	$-j\,2.4226$e+00	$-j\,2.4226$e+00	1.0345e-07
TE$^\zeta_{50}$	$-j\,3.1196$e+00	$-j\,3.1196$e+00	4.9971e-07
TE$^\zeta_{60}$	$-j\,3.8018$e+00	$-j\,3.8018$e+00	8.2061e-07
TE$^\zeta_{70}$	$-j\,4.4759$e+00	$-j\,4.4759$e+00	3.3375e-06
TE$^\zeta_{80}$	$-j\,5.1451$e+00	$-j\,5.1451$e+00	4.7374e-06
TE$^\zeta_{90}$	$-j\,5.8112$e+00	$-j\,5.8112$e+00	2.0576e-05
TE$^\zeta_{10,0}$	$-j\,6.4750$e+00	$-j\,6.4750$e+00	2.9381e-05

3.2.5
Dielectric-Filled Bend Waveguide

We now investigate the effect of filling an H-plane bend waveguide with $R/a = 1$ defined in previous section with a dielectric material with $\epsilon = \epsilon_0\,\epsilon_r$. The FIT solver of CST Studio Suite [24] was used to compute the longitudinal wavenumber of an equivalent waveguide that emulates the curved one. Please see [12] for further details. The first normalized longitudinal wavenumbers obtained by our method (with $M = 15$) were compared against the exact (reference) [12] and by the FIT for $\epsilon_r = \{2, 4, 6\}$, are shown in Tables 3.11–3.16. The relative error was computed using the solution from [12] as a reference. Good agreement is observed for the first modes in all methods.

As a benchmark for the computational cost, the CPU time required to calculate the first 5 modes for the waveguide of last scenario with $\epsilon_r = 6$ was 0.324 s using the solution from [12] using double-precision Fortran code running on a regular laptop. The present method took 0.23 s to run our Matlab code on a regular laptop to compute 15 modes, where the relative error on the fifth modes as 7.26e-4%, as shown in Table 3.16. In contrast, FIT results took 478 s to solve the same problem using a dedicated HP Z820 Workstation with a six-core 2.10-GHz Intel Xeon CPU E5-2620 v2 processor. Note that the FIT results use only the port modes with the standard options with a discretization of 100 hexahedral cells per wavelength in the FIT solver of CST [24]. Although this finely-discretized lattice, the accuracy of FIT deteriorates for high-order modes in the waveguide with $\epsilon_r = 6$.

When small relative errors are acceptable, the computational time of our proposed method is comparable to that of the exact method presented in [12]. Moreover, our variational formulation enables the characterization of waveguides filled with lossy media, which is not possible using the method in [12]. As examples of this flexibility, Tables 3.17 and 3.18 shows the first normalized longitudinal wavenumbers obtained by our method (with $M = 15$) when $\epsilon_r = 6$ and $\sigma = \{10^{-4}, 10^{-3}\}$ S/m. Note that this lossy configuration only changes the complex-valued permittivity that now becomes $\epsilon = \epsilon_0\,\epsilon_r - j\sigma/\omega$. Since ϵ (and the associated wavenumber k) appears outside of the constituent integrals of our method, the CPU time is almost the same of that of the lossless scenarios.

Table 3.11: Normalized longitudinal wavenumbers k_ζ/k in an H-plane bend waveguide (with $R/a = 1$) filled with a material with $\epsilon_r = 2$ obtained by exact (reference) solution [12] and by FIT.

Mode	Ref. [12]	FIT from [24]	Rel. error (%)
TE_{10}^{ζ}	9.1384e-01	9.1384e-01	2.4488e-04
TE_{20}^{ζ}	3.4188e-01	3.4189e-01	2.3565e-03
TE_{30}^{ζ}	$-j\,8.6045$e-01	$-j\,8.6043$e-01	2.4484e-03
TE_{40}^{ζ}	$-j\,1.4031$e+00	$-j\,1.4031$e+00	3.3527e-03
TE_{50}^{ζ}	$-j\,1.8874$e+00	$-j\,1.8873$e+00	4.7393e-03

Table 3.12: Normalized longitudinal wavenumbers k_ζ/k in an H-plane bend waveguide (with $R/a = 1$) filled with a material with $\epsilon_r = 2$ obtained by exact (reference) solution [12] and by our method with $M = 15$.

Mode	Ref. [12]	Our method	Rel. error (%)
TE_{10}^ζ	9.1384e-01	9.1384e-01	3.3402e-07
TE_{20}^ζ	3.4188e-01	3.4188e-01	1.8027e-06
TE_{30}^ζ	$-j\,8.6045$e-01	$-j\,8.6045$e-01	6.4313e-05
TE_{40}^ζ	$-j\,1.4031$e+00	$-j\,1.4031$e+00	4.9202e-04
TE_{50}^ζ	$-j\,1.8874$e+00	$-j\,1.8874$e+00	2.4875e-03
TE_{60}^ζ	$-j\,2.3486$e+00	$-j\,2.3489$e+00	1.0716e-02
TE_{70}^ζ	$-j\,2.7979$e+00	$-j\,2.7991$e+00	4.4859e-02
TE_{80}^ζ	$-j\,3.2400$e+00	$-j\,3.2456$e+00	1.7187e-01
TE_{90}^ζ	$-j\,3.6775$e+00	$-j\,3.6988$e+00	5.7881e-01
$TE_{10,0}^\zeta$	$-j\,4.1118$e+00	$-j\,4.1767$e+00	1.5794e+00
$TE_{11,0}^\zeta$	$-j\,4.5438$e+00	$-j\,4.7048$e+00	3.5430e+00
$TE_{12,0}^\zeta$	$-j\,4.9742$e+00	$-j\,5.3091$e+00	6.7324e+00

Table 3.13: Normalized longitudinal wavenumbers k_ζ/k in an H-plane bend waveguide (with $R/a = 1$) filled with a material with $\epsilon_r = 4$ obtained by exact (reference) solution [12] and by FIT.

Mode	Ref. [12]	FIT from [24]	Rel. error (%)
TE_{10}^ζ	1.0341e+00	1.0341e+00	1.1063e-04
TE_{20}^ζ	6.8698e-01	6.8699e-01	6.6766e-04
TE_{30}^ζ	1.6688e-01	1.6694e-01	3.6821e-02
TE_{40}^ζ	$-j\,7.5193$e-01	$-j\,7.5188$e-01	6.0275e-03
TE_{50}^ζ	$-j\,1.1621$e+00	$-j\,1.1620$e+00	6.3429e-03

Table 3.14: Normalized longitudinal wavenumbers k_ζ/k in an H-plane bend waveguide (with $R/a = 1$) filled with a material with $\epsilon_r = 4$ obtained by exact (reference) solution [12] and by our method with $M = 15$.

Mode	Ref. [12]	Our method	Rel. error (%)
TE_{10}^{ζ}	1.0341e+00	1.0341e+00	2.0679e-07
TE_{20}^{ζ}	6.8698e-01	6.8698e-01	3.1409e-06
TE_{30}^{ζ}	1.6688e-01	1.6688e-01	2.1447e-06
TE_{40}^{ζ}	$-j\,7.5193$e-01	$-j\,7.5193$e-01	1.9779e-04
TE_{50}^{ζ}	$-j\,1.1621$e+00	$-j\,1.1621$e+00	1.4137e-03
TE_{60}^{ζ}	$-j\,1.5233$e+00	$-j\,1.5234$e+00	6.9606e-03
TE_{70}^{ζ}	$-j\,1.8634$e+00	$-j\,1.8640$e+00	3.1816e-02
TE_{80}^{ζ}	$-j\,2.1918$e+00	$-j\,2.1947$e+00	1.3144e-01
TE_{90}^{ζ}	$-j\,2.5130$e-01	$-j\,2.5250$e+00	4.7787e-01
$\mathrm{TE}_{10,0}^{\zeta}$	$-j\,2.8293$e+00	$-j\,2.8687$e+00	1.3932e+00
$\mathrm{TE}_{11,0}^{\zeta}$	$-j\,3.1423$e+00	$-j\,3.2454$e+00	3.2824e+00
$\mathrm{TE}_{12,0}^{\zeta}$	$-j\,3.4527$e+00	$-j\,3.6748$e+00	6.4349e+00

Table 3.15: Normalized longitudinal wavenumbers k_ζ/k in an H-plane bend waveguide (with $R/a = 1$) filled with a material with $\epsilon_r = 6$ obtained by exact (reference) solution [12] and by FIT.

Mode	Ref. [12]	FIT from [24]	Rel. error (%)
TE_{10}^{ζ}	1.0924e+00	1.0924e+00	1.2459e-05
TE_{20}^{ζ}	7.9239e-01	7.9240e-01	8.2146e-04
TE_{30}^{ζ}	5.2127e-01	5.2129e-01	3.5325e-03
TE_{40}^{ζ}	$-j\,3.3334$e-01	$-j\,3.3326$e-01	2.2357e-02
TE_{50}^{ζ}	$-j\,7.8895$e-01	$-j\,7.9229$e-01	4.2388e-01

Table 3.16: Normalized longitudinal wavenumbers k_ζ/k in an H-plane bend waveguide (with $R/a = 1$) filled with a material with $\epsilon_r = 6$ obtained by exact (reference) solution [12] and by our method with $M = 15$.

Mode	Ref. [12]	Our method	Rel. error (%)
TE_{10}^ζ	1.0924e+00	1.0924e+00	4.9454e-07
TE_{20}^ζ	7.9239e-01	7.9239e-01	8.4594e-07
TE_{30}^ζ	5.2127e-01	5.2127e-01	1.6828e-05
TE_{40}^ζ	$-j\,3.3334$e-01	$-j\,3.3334$e-01	3.9641e-05
TE_{50}^ζ	$-j\,7.8895$e-01	$-j\,7.8895$e-01	7.2593e-04
TE_{60}^ζ	$-j\,1.1234$e+00	$-j\,1.1234$e+00	4.3606e-03
TE_{70}^ζ	$-j\,1.4231$e+00	$-j\,1.4234$e+00	2.2097e-02
TE_{80}^ζ	$-j\,1.7059$e+00	$-j\,1.7076$e+00	9.8779e-02
TE_{90}^ζ	$-j\,1.9787$e-01	$-j\,1.9864$e+00	3.8886e-01
$\text{TE}_{10,0}^\zeta$	$-j\,2.2451$e+00	$-j\,2.2724$e+00	1.2163e+00
$\text{TE}_{11,0}^\zeta$	$-j\,2.5070$e+00	$-j\,2.5828$e+00	3.0228e+00
$\text{TE}_{12,0}^\zeta$	$-j\,2.7657$e+00	$-j\,2.9352$e+00	6.1312e+00

Table 3.17: Normalized longitudinal wavenumbers k_ζ/k in an H-plane bend waveguide (with $R/a = 1$) filled with a lossy material with $\epsilon_r = 6$ and $\sigma = 10^{-4}$ S/m obtained by our method with $M = 15$.

Mode	$\Re e(k_\zeta/k)$	$\Im m(k_\zeta/k)$
TE_{10}^ζ	1.0924e+00	-4.0326e-06
TE_{20}^ζ	7.9239e-01	-7.0188e-06
TE_{30}^ζ	5.2127e-01	-1.4001e-05
TE_{40}^ζ	3.9968e-05	-3.3334e-01
TE_{50}^ζ	2.7386e-05	-7.8895e-01
TE_{60}^ζ	2.8098e-05	-1.1234e+00
TE_{70}^ζ	3.0396e-05	-1.4234e+00
TE_{80}^ζ	3.3284e-05	-1.7076e+00
TE_{90}^ζ	3.6585e-05	-1.9864e+00
$\text{TE}_{10,0}^\zeta$	4.0361e-05	-2.2724e+00

Table 3.18: Normalized longitudinal wavenumbers k_ς/k in an H-plane bend waveguide (with $R/a = 1$) filled with a lossy material with $\epsilon_r = 6$ and $\sigma = 10^{-3}$ S/m obtained by our method with $M = 15$.

Mode	$\Re e(k_\varsigma/k)$	$\Im m(k_\varsigma/k)$
$\text{TE}_{10}^{\varsigma}$	1.0924e+00	-4.0326e-05
$\text{TE}_{20}^{\varsigma}$	7.9239e-01	-7.0188e-05
$\text{TE}_{30}^{\varsigma}$	5.2127e-01	-1.4001e-04
$\text{TE}_{40}^{\varsigma}$	3.9968e-04	-3.3334e-01
$\text{TE}_{50}^{\varsigma}$	2.7386e-04	-7.8895e-01
$\text{TE}_{60}^{\varsigma}$	2.8098e-04	-1.1234e+00
$\text{TE}_{70}^{\varsigma}$	3.0396e-04	-1.4234e+00
$\text{TE}_{80}^{\varsigma}$	3.3284e-04	-1.7076e+00
$\text{TE}_{90}^{\varsigma}$	3.6585e-04	-1.9864e+00
$\text{TE}_{10,0}^{\varsigma}$	4.0361e-04	-2.2724e+00

4
Conclusions

In this concluding chapter, we will provide a comprehensive review and summary of the topics covered in this work. We will also offer comments on the results obtained and propose potential directions for future research.

On Chapter 2, we developed a variational formula in toroidal coordinates for curved waveguides with uniform cross-section. The development of an analytic and computational methodology for modeling electromagnetic fields in toroidal coordinates of curved rectangular waveguides with uniform cross-section was presented in Chapter 3, applying the variational formula presented via the Rayleigh-Ritz method in an H-Plane Bend curved rectangular waveguide.

In conclusion, the development of a variational formulation of Maxwell's equations using the Rayleigh-Ritz method for the toroidal coordinate system has provided an efficient solution to the increasing demand for compact devices that can propagate guided waves in curved structures, which is a common requirement in the design of antennas, microwave devices, and filters. The analytical and computational methodology developed in this study offers a means of modeling electromagnetic fields in toroidal coordinates of curved rectangular waveguides with uniform cross-section, using a variational formula via the Rayleigh-Ritz method. This methodology achieved good accuracy while requiring a lower computational cost than conventional *brute force* numerical techniques such as finite elements, finite differences or finite volumes, making it an attractive option for researchers and engineers in the field of electrical engineering. Overall, this research has significant potential applications in the field of engineering and offers a promising direction for future studies.

An important point regarding the computational resources was that our method requires a CPU time comparable to that of the exact method presented in [12]. As an advantage, the present method does not requires the employment of specifically designed cylindrical functions with complex-valued orders and real-valued arguments as in [12], being more flexible to be implemented in any computational language that supports basic linear algebra system. In addition, our variational formulation enables the characterization of waveguides filled with lossy media without additional cost.

For future research, we recommend exploring the application of this method to other geometries of waveguides, in addition to the curved rectangular waveguides studied in this research. Additionally, investigating the use of the sources of current proposed in the variational formulation presented in this study could further enhance the accuracy and efficiency of the methodology. Such investigations could provide valuable insights and expand the scope of applications of the proposed methodology in the field of electrical engineering.

Bibliography

[1] R. F. Harrington, *Time-Harmonic Electromagnetic Fields*. New York, NY, USA: McGraw-Hill, 1961.

[2] L. Lewin, D. Chang, and E. Kuester, *Electromagnetic waves and curved structures*. London, UK: Peter Peregrinus, 1977.

[3] J. A. Cochran and R. G. Pecina, "Mode propagation in continuously curved waveguides," *Radio Science*, vol. 1, no. 6, pp. 679–696, 1966.

[4] C. J. Chapman, "The asymptotic theory of dispersion relations containing bessel functions of imaginary order," *Proceedings of the Royal Society A: Mathematical, Physical and Engineering Sciences*, vol. 468, no. 2148, pp. 4008–4023, 2012.

[5] A. Weisshaar and V. Tripathi, "Perturbation analysis and modeling of curved microstrip bends," *IEEE Trans. Microw. Theory Techn.*, vol. 38, no. 10, pp. 1449–1454, 1990.

[6] X.-S. Fang and Z.-Q. Lin, "A coupled-mode approach to the analysis of fields in space-curved and twisted waveguides," *IEEE Transactions on Microwave Theory and Techniques*, vol. 35, no. 11, pp. 978–983, 1987.

[7] M. Mongiardo, A. Morini, and T. Rozzi, "Analysis and design of full-band matched waveguide bends," *IEEE Trans. Microw. Theory Techn.*, vol. 43, no. 12, pp. 2965–2971, 1995.

[8] B. Gimeno and M. Guglielmi, "Multimode equivalent network representation for h- and e-plane uniform bends in rectangular waveguide," *IEEE Trans. Microw. Theory Techn.*, vol. 44, no. 10, pp. 1679–1687, 1996.

[9] A. Weisshaar, S. Goodnick, and V. Tripathi, "A rigorous and efficient method of moments solution for curved waveguide bends," *IEEE Trans. Microw. Theory Techn.*, vol. 40, no. 12, pp. 2200–2206, 1992.

[10] P. Cornet, R. Dusseaux, and J. Chandezon, "Wave propagation in curved waveguides of rectangular cross section," *IEEE Trans. Microw. Theory Techn.*, vol. 47, no. 7, pp. 965–972, 1999.

[11] C. S. Lavranos and G. A. Kyriacou, "Eigenvalue analysis of curved waveguides employing an orthogonal curvilinear frequency-domain finite-difference method," *IEEE Trans. Microw. Theory Techn.*, vol. 57, no. 3, pp. 594–611, 2009.

[12] G. S. Rosa, "An accurate and numerically stable formulation for computing the electromagnetic fields in uniform bend rectangular waveguides," *IEEE Transactions on Microwave Theory and Techniques*, vol. 71, no. 3, pp. 988–996, 2023.

[13] Y. Wang and D. Dai, "Ultra-sharp multimode waveguide bends with dual polarizations," *J. Lightw. Technol.*, vol. 38, no. 15, pp. 3994–3999, 2020.

[14] W. Lui, C.-L. Xu, T. Hirono, K. Yokoyama, and W.-P. Huang, "Full-vectorial wave propagation in semiconductor optical bending waveguides and equivalent straight waveguide approximations," *J. Lightw. Technol.*, vol. 16, no. 5, pp. 910–914, 1998.

[15] X. Wu and J. Xiao, "Full-vector analysis of bending waveguides by using meshless finite cloud method in a local cylindrical coordinate system," *J. Lightw. Technol.*, vol. 39, no. 22, pp. 7199–7209, 2021.

[16] Z. Han, P. Zhang, and S. I. Bozhevolnyi, "Calculation of bending losses for highly confined modes of optical waveguides with transformation optics," *Opt. Lett.*, vol. 38, no. 11, pp. 1778–1780, Jun 2013.

[17] E. Lezar and D. B. Davidson, "Electromagnetic waveguide analysis," in *Automated Solution of Differential Equations by the Finite Element Method*, ser. Lecture Notes in Computational Science and Engineering, A. Logg, K.-A. Mardal, and G. Wells, Eds. Berlin, Heidelberg: Springer, 2012, vol. 84.

[18] G. S. Rosa, "Pseudo-analytical modeling for electromagnetic well-logging tools in complex geophysical formations," Ph.D. dissertation, Dept. Elect. Eng., Pontifical Catholic University of Rio de Janeiro, Rio de Janeiro, RJ, Brazil, 2017.

[19] G. S. Rosa, J. R. Bergmann, and F. L. Teixeira, "A perturbation method to model electromagnetic well-logging tools in curved boreholes," *IEEE Trans. Geosci. Remote Sens.*, vol. 56, no. 4, pp. 1979–1993, Apr. 2018.

[20] K. B. Petersen and M. S. Pedersen, "The matrix cookbook," , Tech. Rep., 2012, version November 15, 2012. [Online]. Available: https://www.math.uwaterloo.ca/~hwolkowi/matrixcookbook.pdf

[21] C. A. Balanis, *Advanced Engineering Electromagnetics*, 2nd ed., ser. IEEE Press Series on Electromagnetic Wave Theory. Wiley, 2012.

[22] J. A. Stratton, *Electromagnetic Theory*. New York, US: Wiley-IEEE Press, 2006.

[23] MATLAB, *version 9.11.0.1687835 (R2021b) Prerelease*. Natick, Massachusetts: The MathWorks Inc., 2021.

[24] CST AG, CST Studio Suite 2019, Darmstadt, Germany, 2019.